The "New" Science of "Complex Fluids"

William M. Gelbart*

Department of Chemistry and Biochemistry, The University of California, Los Angeles, Los Angeles, California 90024

Avinoam Ben-Shaul

Department of Physical Chemistry and The Fritz Haber Research Center, The Hebrew University of Jerusalem, Jerusalem 91904, Israel

Received: February 29, 1996; In Final Form: April 23, 1996[⊗]

We present an overview of the modern study of complex fluids which, because of the overwhelming breadth and richness of this field, unavoidably neglects many interesting systems and research developments. In proposing a definition of the field, we discuss first the special role played by phenomenological theory and the limitations of molecular-level description. The remainder of the article is organized into sections which treat model colloids, micellized surfactant solutions, interfacial films and microemulsions, bilayers and membranes, and new materials. In each instance we try to provide a physical basis for the special nature of interactions and long-range ordering transitions in these novel colloidal and thin layer systems. At the heart of understanding these highly varied phenomena lie the curvature dependence of surface energies and the coupling between self-assembly on small length scales and phase changes at large ones.

1. Introduction

1.1. What Are Complex Fluids? In this Introduction we suggest several answers to the following questions: What are complex fluids? Why are they important? And how are they unique, e.g., what new scientific and conceptual challenges do they pose? Then, in the sections which follow, we briefly review recent theoretical and experimental work in particular complex fluid areas and pose some of the current unsolved problems in each of these domains. Without making any attempt to be exhaustive, we will compare and contrast the basic features of colloidal suspensions, micellar solutions, surfactant monolayers and microemulsions, vesicles and model cell membranes, and new "soft, condensed" materials. While we shall insist on including polymer solutions as an especially important example of complex fluids, we do not discuss them at any length here since they are treated separately in the article by Lodge and Muthukumar.

Perhaps the first definition of a complex fluid which comes to mind is simply "a fluid made up of a lot of different kinds of stuff". While this description certainly applies to most of the above examples, it also includes systems, such as molecular mixtures comprised of similarly sized components (e.g., liquid benzene/toluene/hexane), which we do *not* consider to be complex fluids. Also, even though *self-assembly* is a crucial ingredient for understanding micellar solutions and microemulsions, it is *not* directly relevant to polymer solutions or to "ordinary" colloidal suspensions of particles with fixed molecular weight and composition. Instead, we suggest that the common, defining feature of a complex fluid is *the presence of a mesoscopic length scale* which necessarily plays a key role in determining the properties of the system. By mesoscopic size we mean intermediate between molecular and macroscopic [Greek *mesos* middle]. For the kinds of examples mentioned in the first paragraph, the mesoscopic scale is as follows: the length, say, of micellar rods, generally tens of nanometers; the Flory radius (persistence length) of flexible (wormlike) chains in polymer solutions, typically tens to hundreds of nanometers; the radii of microemulsion drops or vesicles or the dimensions of colloidal spheres or rods, again on the order of 10−100 nm; the pore (bubble) size in aerogels (foams); the size of heterogeneities in block copolymer systems and molecular composites; and the film thickness of organic multilayers.

In the various sections of this article we will consider all of the above systems and their mesoscopic length scales in considerable detail. In the case of the self-assembling systems, e.g., micellar solutions and microemulsions, where the interacting particles are themselves aggregates of large numbers of amphiphilic molecules, we will need to address directly how these characteristic lengths arise as a consequence of the hydrophobic effect, the competing demands of the molecular polar head groups and alkyl chains for cross-sectional space, and the curvature energy of interfacial films of surfactant. On the other hand, in the case of polymer solutions and "ordinary" colloidal solutions, the size of the particles follows directly from their *fixed* molecular weights. In *both* cases, however, the characteristic properties of these complex fluids are due to the mesoscopic scale of their basic particles. The rheological behavior, for example, is almost always "anomalous", e.g., nonlinear, because the viscous torques exerted on the particles by even very small velocity gradients are quite large. Similarly, the electric, magnetic, and optical responses are invariably "strong", again because of the *supra*molecular (mesoscopic) scale of the fluid.

The practical importance of complex fluids has been appreciated for a long time, starting well before their study could be systematically included in the fundamental theoretical and experimental programs of physical science. After all, most (all?) biological and geological fluids (e.g., blood, cell cytoplasm, mud, and sea water) are colloidal suspensions of one kind or another, and similarly for paints, liquid foodstuffs, etc. Micellized surfactants provide the bases for a broad class of detergent and cosmetic formulations and industrial processes. As far as commercial applications are concerned, polymers are the most important and all-pervasive class of synthetic materials because

[⊗] Abstract published in *Advance ACS Abstracts,* July 1, 1996.

S0022-3654(96)00657-0 CCC: $12.00 © 1996 American Chemical Society

of their incredible range of structural, rheological, optical, and even electronic properties. Still more dramatically, and fundamentally, vesicles (closed bilayers) of phospholipids provide the basic models for biological cell membranes, while biopolymers (proteins, DNA) are the very "molecules of life".

Because of this overwhelming practical usefulness and natural abundance, complex fluid systems have long formed a cornerstone for scientific inquiry. The reason we entitle our article "The *New* Science of Complex Fluids" is because—until quite recently—few attempts were made to treat systems such as colloidal suspensions, or micellar and polymer solutions, with modern physical chemical ideas and techniques. By the 1960s, for example, it was quite common for high-resolution spectroscopies (UV, optical, infrared, and microwave) to be used successfully in determining the properties of individual molecules either in the gas phase or in liquid solutions of simple solvents. Similarly, magnetic resonance methods (NMR, ESR) were providing comparably detailed information about molecular structure and dynamics. A wide panoply of particle (electron, neutron) and radiation (light, X-ray) scattering techniques were already being applied to probing the interatomic correlations in simple fluids and biological macromolecules. But complex fluid systems were essentially untouched by this revolution in experimental structural determination. Rather, they were still being studied almost exclusively by *bulk* probes such as turbidity, viscosity, and osmotic pressure measurements. Static ("elastic") light scattering experiments, inspired by the work of Debye,[1] allowed for fairly accurate estimates of molecular weight and aggregation number in dilute polymer and micellar solutions. But it was not until the advanced development of the laser and, in particular, of the optical analogues of (microwave) homo- and heterodyne detection that dynamic ("quasi-elastic") light scattering made possible much more detailed inferences about the sizes and shapes of macromolecules and molecular aggregates.[2] Perhaps even more significantly, small-angle X-ray and neutron scattering methods, in particular the technique of contrast variation,[3] led to almost-angstrom resolution in determining the structures of these systems. At the same time, partial deuteration in NMR studies led to direct information about, for example, individual C−C bond orientational order in alkyl chain "tails" of surfactant molecules in micelles and bilayers.[4] By the 1980s, aqueous solutions of micelles and of macromolecules were successfully vitrified[5,6] without disruption of their complex fluid structures, thereby facilitating the first truly reliable electron micrograph pictures of these highly delicate colloids. Finally, surface force microscopy has made possible the direct measurement of the potentials of interaction between model colloidal particles, at distances down to just a few angstroms,[7] testing not only the classic DLVO theory but also much more recent ideas, such as those of hydration and polarization forces.

Equally significantly, the ushering of complex fluids research into the modern era of physical chemistry has come about because of dramatic new advances in statistical mechanics and many-body theory. To appreciate these issues, it is useful to make some general remarks about the differences in motivation and appropriateness of molecular-level vs phenomenological theory.

1.2. Problems with Molecular Approaches. Let us consider, for purposes of illustration, the basic problem of the spontaneous appearance of micelles above a threshold concentration of surfactant in water and the subsequent evolution of these aggregates into larger ones as the concentration is raised still further. The relevant experimental situation is that (i) surfactant molecules are only slightly soluble in water, due to their long hydrocarbon chains, and (ii) at their limit of solubility, called the critical micelle concentration (cmc), the surfactant molecules do not form a *bulk* phase in coexistence with water (as do the usual oils, that is, long hydrocarbon chains without polar heads) because their strongly hydrophilic ends need to be in contact with water. Instead, they organize into finite aggregates—*micelles*—which allow the hydrophobic effect to be satisfied; i.e., the water is shielded from the surfactants' "tails" and allowed simultaneously to hydrate their "heads". For typical surfactants, this micellization occurs at concentrations so low that the volume fraction of water is almost one. Accordingly, the micellar aggregates are essentially unaware of one another: more explicitly, the interactions between them can be neglected and their solution treated as ideal. Nevertheless, as we shall see explicitly in the simple statistical thermodynamic theory described in the following section, as the surfactant concentration is raised above the cmc, a familiar observed scenario is that the average size of the micelle *increases*! Immediately, one is confronted with a qualitative phenomenon which needs to be explained and understood: *the equilibrium states of a micellar solution, corresponding to successively higher surfactant concentrations, involve average aggregation numbers which increase with concentration*. Note that in the case of "oridinary" colloidal suspensions, such as dilute solutions of synthetic polymers or biomolecules, the aggregation number (molecular weight) is *fixed*, and the only statistical mechanical problem which needs to be solved is that of calculating the bulk properties of the solution as a function of concentration, temperature, and molecular weight. How, then, does one go about accounting theoretically for both the onset of micellization and the subsequent evolution of average aggregation number upon increasing the overall *volume* fraction of surfactant?

The most conceptually straightforward, and apparently "rigorous", approach is simply to treat this complex fluid system as if it were a simple one. More explicitly, we consider a large number of surfactant and water molecules, corresponding to a concentration just below what we expect for the cmc, and we write down intermolecular potentials that describe the interactions between water−water, water−surfactant, and surfactant−surfactant pairs, taking into account all possible separation vectors, internal conformations, and relative orientations. We then carry out a molecular dynamics simulation for this concentration and for, say, room temperature, starting with a random, mixed configuration of all the molecules. Upon equilibrating the system, we average over the ensemble of configurations to determine the distribution of aggregates, expecting to find that the surfactants have essentially remained as monomeric, *un*micellized species. We now perform a similar computation for each of successively higher concentrations until we can identify the cmc, i.e., the concentration at which, say, half of the equilibrated surfactant molecules are identified with micellar aggregates and the other half with monomer form. Finally, we continue to carry out simulations at each of still higher concentrations, computing for each equilibrium the average aggregation number of the micelles.

Now, *what is wrong with this picture*?! First, of all, we have to consider how long it takes for the above system to come to equilibrium when the concentration lies above the cmc. The fact is that milliseconds, *and longer times*, are required. This corresponds to the fact that any given surfactant molecule "pops" out of its micelle after a "residence time" of about a microsecond. Since hundreds to thousands of molecules typically comprise an aggregate, this means that times on the order of milliseconds are associated with the breakup of one micelle and formation of another. And these are precisely the dynamical

events that are needed to establish (surfactant exchange) equilibrium in the system. Note that the size distribution of micelles is independent of time, even as the individual surfactant molecules are continually exchanging between aggregates, just as the amounts of gas and liquid phases in coexistence at boiling are constant even as their molecules are exchanging via evaporation and condensation processes. So, we are confronted with the problem of performing molecular dynamics simulations for times as long as milliseconds, i.e., for times about *6 orders of magnitude* longer than currently feasible on available machines.

There is a second problem. Suppose we consider now the *number* of molecules needed to carry out the above simulation. Typical cmc values correspond to surfactant mole fractions of about 10^{-5}. But to form a micelle with an aggregation number even as small as 100 surfactant molecules would then require as many as 10^5 times more water molecules, i.e., as many as 10^7 water molecules—more than can presently be handled by the most ambitious calculations on the most powerful computers. Furthermore, recall that molecular dynamics simulation of this number of molecules needs to be performed not for picoseconds or nanoseconds, but for times up to a million times longer!

Finally, surfactants are highly complicated molecules whose interactions in aqueous solution are not well-known; accordingly, many calculated properties in atomistic level computations can be quite sensitive to these unresolved details. Nevertheless, by equilibrating a *pre*assembled aggregate involving a *fixed* number of surfactant molecules, much useful information has been obtained about the conformational structures and dynamics of micellar interiors (see discussion in section 3.2).

1.3. The Case for Phenomenological Theories. The point of this discussion has been to make clear the importance of pursuing an approach quite different from the "simple" molecular one in setting out to explain the behavior of even highly dilute solutions of surfactant in water. At higher concentrations, where the volume fraction of surfactant (and hence of micelles, far above the cmc) is no longer negligible compared to one, we must complicate the situation further by taking into account interactions between the aggregates. This, in turn, gives rise to several new phenomena, namely, changes in not only average aggregation number (upon increase in concentration) but also micellar shape and long-range orientational and positional order of the aggregates. If a molecular level description was not feasible or appropriate in the dilute, ideal, solution limit, it surely will fail still more dramatically at these higher concentrations. This conclusion becomes even more compelling when we consider the important role which *defects* play in ordered, concentrated phases of surfactant in water. For example, many surfactants which form small cylindrical micelles just above the cmc are observed to form lamellar phases at high volume fractions; i.e., they organize as stacked bilayers. But the bilayers are riddled by "holes" and "cracks", with densities and shapes and patterns which vary with overall concentration and temperature. Sometimes the lamellar phase actually consists not of these stacked bilayers, but rather of layers of small finite pieces of bilayer ("disks" and "ribbons", say), much like the smectic A phase commonly observed in *neat*, one-component "thermotropic" liquids of anisotropic molecules. Furthermore, when an additional amphiphilic species—"cosurfactant"—is added, the structural evolution and phase behavior become even richer. A systematic prediction of all of these possible scenarios, as a function of concentration, temperature, and *composition*, is clearly well outside the realm of feasibility of a molecular theory.

So how can we proceed? We argue that a phenomenological statistical thermodynamic approach is required, and we shall give several explicit examples of how such a theory is formulated and discuss how and why it works. We will feature statistical thermodynamic descriptions in which the starting point is often provided by a free energy rather than an explicit Hamiltonian. An important exception is that of the various spin and lattice Hamiltonian approaches which have proved so useful in accounting for the low interfacial tensions and the phase behaviors of model microemulsions; see section 4. Another exception involves the recent studies of micellar systems via molecular dynamics[8] and Monte Carlo[9] simulations based on site−site interactions between the "water-like" and "oil-like" monomers comprising amphiphilic species. But it is important to note that these interaction energies are purely phenomenological, not to be confused with the atomistic potentials referred to above in our discussion of molecular theories. More explicitly, a single energy parameter is introduced to describe the preference for like−like ("water−water" or "oil−oil") interactions. The quotation marks for "water" and "water-like" (and similarly for "oil" and "oil-like") remind us that a "water" monomer can refer alternately to both actual water molecules and, say, a carboxylate ion or zwitterionic phosphate/ammonium head group, etc.; also, structural effects such as hydrogen bonding, counterion binding, and other internal (e.g., conformational) degrees of freedom have *not* been included. Nevertheless, it is possible in this way to observe on the computer the spontaneous micellization of amphiphilic species and to correlate the associated cmc and aggregation number with relative sizes of head and tail regions[8,9] and with bulk oil−water interfacial tensions.[8] More interestingly, the increase with concentration of average micellar size, and the onset of long-range orientational and positional ordering and appearance of new structures (e.g., lamellae with defects) at still higher concentrations, have been beautifully demonstrated[9] for a wide variety of model amphiphilic species, i.e., chain molecules consisting of different relative numbers of water-like and oil-like monomers. Again, we emphasize that these calculations are useful in spite of, or (more precisely) *because of*, their being phenomenological rather than molecular in their level of description.

In addition to the micellar examples referred to above, we shall concentrate on the cases of oil−surfactant−water microemulsion systems, where the structures and phases range from simple dispersions of droplets to bicontinuous "sponge" states and of phospholipid + detergent solutions in which the aggregates evolve from vesicles to micelles at low concentrations and from lamellar to hexagonal phases at high volume fractions. In each of these examples we will argue that the relevant phenomenological theory serves to provide highly useful predictions of structures and phase behavior and thereby to explain the basic physics underlying them for a wide range of surfactant-in-water systems. In some instances the theory does not even attempt to provide an explicit Hamiltonian, but starts instead with physically suggestive forms for the several free energy terms which describe the "self-energy" of micelles, the interaggregate interactions, the contributions from the entropies of dispersion and of "packing", and the effects of long-range orientational and positional ordering. In other cases, we do insist on starting with a Hamiltonian, but it is distinctly not atomistic/microscopic in origin; i.e., it is not couched in terms of molecular-level interactions. Rather, it might take as its fundamental unit the "minimum micelle" and include all interactions between these objects, thereby allowing for a systematic treatment of micellar structural evolution and phase

behavior. The Hamiltonian is itself "phenomenological", in much the same spirit as the Ising and lattice-gas Hamiltonians[10] provide highly satisfactory accounts of the ferromagnetic transition, and gas−liquid condensation and binary fluid/alloy phase separations without any truly microscopic ingredients being necessary (or desirable!). An advantage of the phenomenological Hamiltonian vs statistical thermodynamic free energy formulation is that one can straightforwardly and systematically go beyond mean-field approximations, either analytically with renormalization group theory, say, or numerically with, for example, Monte Carlo simulation.

2. Colloidal Suspensions

Like so many other subfields of complex fluids, the area of colloidal suspensions is incredibly broad and rich. Indeed, we have already stressed in the Introduction that essentially *all* fluids are colloidal suspensions, whether we are thinking about tap water (yup, sorry!), blood, mud, polymer solutions, paint, cell cytoplasm, etc. So, instead of trying in any way to cover this vast spectrum, we will rather arbitrarily confine ourselves to just a few examples which provide especially good opportunities for making connections between relatively familiar ideas in classical statistical mechanics on one hand and different areas of complex fluids, materials science, and even biology on the other.

2.1. Hard Spheres and Freezing. Certainly the simplest, most widely treated, and best characterized model colloid is that of "hard spheres". This system had been the subject of an extraordinary amount of theoretical investigation, for many decades, because of the crucial role it plays in understanding the structure of *simple* fluids. After all, the century-old idea of van der Waals posits that the structure of a simple fluid is dominated by short-range, repulsive, interactions; the longer ranged, slowly varying attractions contribute primarily to the thermodynamic properties in mean-field approximation.[10,11] Accordingly, dozens of theories of the hard-sphere "reference system" have been formulated, for both its structure and its thermodynamics with attractions being included via various perturbation treatments.[12] It was only much more recently, however, that experimental efforts were concentrated on the development of laboratory examples of the "hard-sphere fluid". The first challenge was to make particles which were sufficiently monodisperse and the second to render them purely repulsive in their mutual interactions. The first problem was solved via emulsion polymerization processes, involving polystyrene (PS) or poly(methyl methacrylate) (PMMA), which result in spheres in the micron and submicron range having at most a few percent size dispersion. The second goal, which essentially amounts to keeping the "polyballs" far enough apart not to be dispersionally attracted to one another, is achieved by coating the balls with a high density of flexible polymers which lead to entropic repulsions between the particles because of the large number of chain conformational states which become inaccessible at short separation distances. Measurements of the osmotic pressure and compressibility, for example, demonstrate a dramatic agreement with predicted hard sphere properties.[13] And similarly for the radial distributions measured from inversion of scattering structure factors and from direct, real-space imaging of particle positions from confocal microscopy.[14]

Even more interestingly, much work has been focused on the *phase* behavior of these model colloid systems. Early theoretical work, notably computer simulations in the 1950s and 1960s, established the remarkable fact that hard spheres undergo a freezing transition, i.e., show a two-phase coexistence involving fluid and solid states at volume fractions of 0.49 and 0.55, respectively.[15] Subsequently, considerable quasi-analytical theory has explained this phenomenon in terms of a competition between entropy loss associated with the onset of long-range order and the ("free volume") entropy gain arising from "relief of gridlock", i.e., from the larger number of packing configurations made possible by the "sorting out of particles" as they are each assigned to their own lattice sites about which they become free to undergo local motions. Recall that because the spheres are "hard"—they exert no forces on one another unless they actually touch, in which case the repulsion is infinite—there is no role played by energy in this problem. Rather, the free energy of the system is comprised entirely of entropy contributions. The key to understanding the stability of crystals over fluids at high volume fractions lies in the fact that the *random* close packing density (dimensionless, volume fraction, $\phi = 0.64$) for hard spheres is significantly smaller than the *hexagonal* close packing value (0.74). Accordingly, before the density becomes high enough for the fluid to run out of packing possibilities (at 0.64), it undergoes a phase transition (at 0.49) to a crystalline state (0.55). Only when the fluid is compressed quickly enough does it "get stuck" as a disordered system, forming a long-lived metastable glassy state around $\phi = 0.58$ which persists up to the random close packing density 0.64.[16] Indeed, one might think of hard sphere freezing as a "glass-avoiding transition". With the development of the PMMA suspensions described above, these features of hard sphere behavior have been beautifully confirmed by experiment.[13]

As soon as the hard sphere suspensions are allowed to enjoy a significant degree of polydispersity, many interesting new phenomena arise. Most notably, the freezing transition disappears as soon as the width of the size distribution exceeds about 10%. In fact, this is not really surprising, since the "gridlock" referred to above in the monodisperse case no longer arises when the spread in particle diameters is large enough: space which would otherwise be "wasted" is now "filled in" because of the continuous range of size. A quite different effect is seen for the case of two, distinct, sizes of particle. The most studied instance here is that of a binary size ratio of 0.58, since this corresponds to a value appropriate to naturally occurring gem opals—crystalline arrays of colloidal silica spheres. For this system it was observed[17] that "superlattices" with stoichiometry AB_2 and AB_{14} arose (A and B referring here to large and small particles, respectively), according to whether the compositions were close to 1:3 or 1:14. It turns out, for this ratio of particle diameters, that these are the structures which can be compressed to volume fractions ($\phi_A + \phi_B$) that exceed the close packing value (0.74) for *mono*disperse spheres: otherwise, phase-separated crystals of pure A and pure B will be more stable as the overall system is concentrated at fixed composition. This picture, inspired directly by nature, has since been nicely confirmed by several computer simulations and density-functional calculations.[18]

An even more exotic phenomenon arises when the ratio of particle sizes differs still more significantly from unity, say by several powers of 10. It is then found that the small spheres give rise to an effective *attraction* between the large ones, even though they all strictly remain "hard" particles. This effect turns out to be essentially equivalent to that of the "depletion" interaction which was postulated earlier for polymer-containing solutions of large colloidal particles.[19] The basic idea is that the effective attraction between the big particles arises from the need for the smaller ones to get out of their way in order to avoid being confined and thereby have their translational entropy lowered.[20] Consistent with the above discussion, one finds that colloidal suspensions of coated PMMA "hard spheres" can show

gas−liquid condensation, as well as fluid−solid transition, if one adds "free" (nonabsorbing) polymer; and by varying the size and concentration of polymer, one can vary both the depth and the range of the effective attraction.[13] An especially beautiful example of this phenomenon of depletion forces is provided by the example of oil-in-water emulsions, with the micron-sized oil drops playing the role of the big particles and nanometer-scale, globular micelles due to added surfactant serving as the small ones.[21] Since the strength of the depletion force can be shown to be proportional to the diameter of the big drops, the largest of the oil drops are most strongly attracted to one another. The result is a condensation/crystallization of the largest drops; since oil is lighter than water, instead of falling out of the solution as precipitate, they "cream" to the top. Skimming off this large-particle fraction and adding surfactant micelles then results in a further fractionation; a few successive cycles of this kind and one obtains a highly monodisperse dispersion of oil drops which, furthermore, is especially stable because of the absence of the usual Ostwald ripening/condensing processes wherein smaller drops sacrifice themselves to larger ones.

2.2. Hard Rods and Orientational Order. A second class of model colloidal system which allows for important tests of simple statistical mechanical ideas is that of the "hard rod". Here the relevant phase transition is the onset of long-range orientational ordering, i.e., the isotropic to liquid transition, and its essential physics was first exposed by Onsager almost 50 years ago.[22] The idea turns out to be intimately related to those underlying the *freezing* transition for hard *spheres* discussed at some length above. Consider a suspension of hard rods, i.e., prolate objects which exert no forces whatsoever on one another until they touch, at which point they experience infinite repulsions. Accordingly, the system is athermal: energetic considerations never enter into the problem, and the free energy consists entirely of entropic contributions. The first entropic term is that arising from the distribution of orientations of the particles, and it favors the isotropic solution in which all rod orientations are equally likely. The second is associated with the number of ways one can pack the hard rods, and it favors the aligned fluid state in which neighboring rods are more likely to be parallel. This is because the volume excluded to one hard rod by another is a minimum when their axes lie along the same direction and a maximum when they are perpendicular. Indeed, that rodlike objects "take up less space"—can pack more efficiently (more ways)—when they are parallel is obvious to anybody who has tried to fit spilled wooden matches back into their box without first aligning them. Since this packing entropy contribution to the free energy involves pairs of particles in lowest order, its dependence on density is quadratic and higher, whereas the orientational term, being a single-particle ("ideal-gas-like") contribution, varies linearly with density. Hence, at high enough concentrations the packing entropy term will dominate, and the overall free energy of the system will be minimized for the aligned fluid state. Onsager showed in particular that this transition should be first order and that for *long* rods the limiting concentration—particle volume fraction—for the stability of the isotropic phase should be of order D/L, where D and L describe the diameter and length of the rods.

This fundamental idea of Onsager has been subjected to many experimental tests, involving aqueous solutions of long, rigid, rodlike, macromolecules such as TMV (tobacco mosaic virus),[23] PBLG (poly(benzyl-1-glutamate)),[24] and DNA.[25] Figure 1 shows an electron micrograph of a solution of TMV particles ($L = 300$ nm and $D = 18$ nm) in their nematic state; here the added salt concentration is low enough so that the electrostatic repulsions between the charged rods are strong enough to swamp the dispersional attractions. Similar systematic studies have been performed as well for inorganic rodlike particles of aluminum oxide sterically stabilized by a coating of polyisobutene.[26] The characteristic optical textures observed between crossed polarizers provide the simplest test for nematic order in these systems.

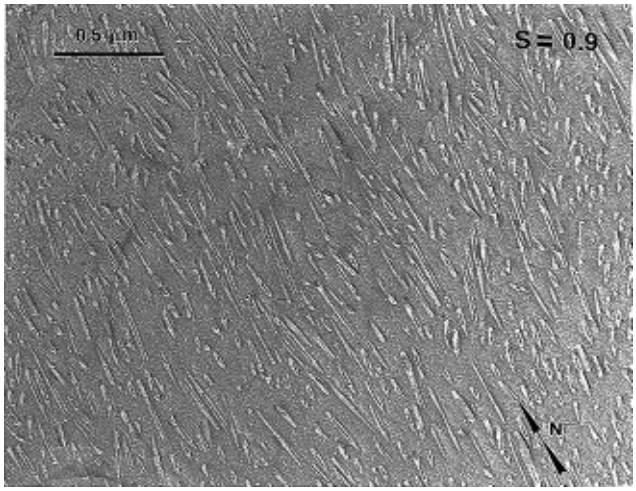

Figure 1. Electron micrograph of the nematic state of an aqueous solution of tobacco mosaic virus (TMV) particles, each with length and width of approximately 300 and 20 nm, respectively. *S* denotes the degree of orientational alignment. Micrograph courtesy of J. A. Zasadzinski.

Also, *smectic* phases of TMV have been reported:[27] here the aligned molecules sit preferentially in layers normal to the nematic direction, but there is no ordering of the centers of mass *within* the layers. Partially (quasi-one-dimensionally) positionally ordered liquid crystals of this kind had long been known in the case of *neat* liquids ("thermotropics"), and a great deal of phenomenological, meanfield, and density-functional theories, as well as computer simulation studies, have been carried out to account for this additional phase.[28] From the work on the thermotropics, where the constituent molecules almost always involve a rigid rodlike core which has either a dipole moment associated with it or flexible end chains attached to both ends, it was long believed that excluded-volume forces of the Onsager type were by themselves not sufficient for a system to show a smectic phase as well as a nematic. And so considerable excitement was generated about 10 years ago when Monte Carlo simulations on aligned hard rods suggested that, for large enough length-to-width ratios, increasing the density of a nematic suspension could lead directly to smectic ordering.[28a] This conclusion was quickly confirmed by a large number of density-functional calculations,[28b−f] and the simple physical picture which emerges is again based on the dominant role played by packing entropy. More explicitly, the rods eventually need to go into layers in order to lower their effective "lateral" density, i.e., so that they can move greater distances (normal to their alignment) before banging into each other and thereby pack more ways; this enhanced entropy is sufficient to offset the entropy loss associated with organizing into layers.

2.3. Flexible Particles. One of the best documented and most elegant examples of the application of modern statistical mechanics to elucidating special features of complex fluids is surely provided by the theory of single-chain polymer structure and phase behavior. These latter issues are addressed in the article by Lodge and Muthukumar elsewhere in this volume. They discuss in particular the random-walk analogy between chain conformation and particle diffusion, the idea of persistence length, the crucial complication of excluded volume ("self-

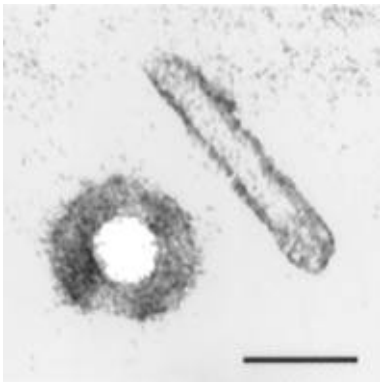

Figure 2. Electron micrograph of toroidal and rodlike particles produced from 1350 base pair fragments of closed circular pUC18 plasmid DNA in aqueous solution (5 μg/mL), upon condensation with the trivalent cation hexaammine cobalt (30 μM). Scale bar = 50 nm. Micrograph courtesy of C. G. Baumann and V. A. Bloomfield.

avoidance"), and the possibility of intramolecular polymer collapse. In completing this present section, we simply call the reader's attention to what is arguably the most important and challenging instance of these phenomena.

Earlier, we casually included DNA along with TMV as examples of colloidal suspensions of biomolecules which undergo the isotropic−nematic transition as systems of repulsive rigid rods. But it is important to note that DNA behaves this way only when its molecular weight is low enough for its length not to exceed a few hundred angstroms. Otherwise, say, for lengths on the order of microns or longer, it behaves like a flexible chain molecule, and entirely different phenomena come into play. A most dramatic example is that of DNA "condensation", a phenomenon which has been very actively studied not only within the context of the coil-to-globule transition in polymer physics[29] but also because of its obvious connection to the biological process whereby DNA goes from solution to chromosomes with a density increase of many orders of magnitude.[30] The condensation from long, flexible chains to high-density particles of precipitate is driven alternately by addition of polyvalent cations or lower-molecular-weight polymers or simply by mixing in a "bad" solvent. In virtually all cases, independent of the source of the DNA (and hence of its genetic information) and of its length (varying upward from hundreds of angstroms to microns), the condensed particles are found[31] to contain approximately the same amount of DNA and to have about the same size (500−1000 Å)! Most often the particles of precipitate are toroidal (with the DNA wound circumferentially), but sometimes they are more rodlike in shape (with the strands wound much as in a "forearm" of yarn): see electron micrographs shown in Figure 2. While several interesting first steps have been attempted,[32] it is clear that more theoretical work will be useful to account for these remarkable physical/biological processes.

In moving on to *self-assembled* systems of colloidal "particles", e.g., micellar aggregates in aqueous solutions of amphiphiles, we shall see that all of the fundamental phase transitions discussed above—for example, the orientational alignments, partial positional orderings, and freezing/crystallizations—are equally important for understanding the bulk behavior of a large variety of other complex fluids. But an *additional* degree of freedom (order parameter) arises, in particular the size and shape of the colloidal aggregates themselves, which must be self-consistently coupled to the usual thermodynamic parameters (concentration, temperature, degree of long-range order) and which thereby enriches significantly the range of phenomena and properties involved.

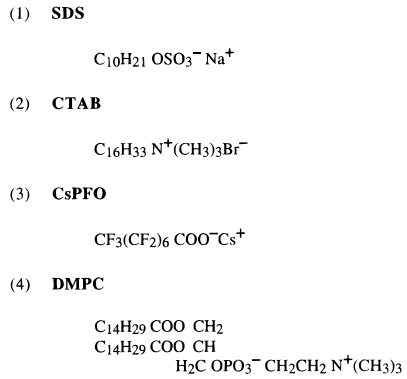

Figure 3. Structural formulas for typical classes of amphiphile: (1) sodium decyl sulfate, SDS; (2) cetyltrimethylammonium bromide, CTAB; (3) cesium perfluorooctanoate, CsPFO; and (4) dimyristoylphosphatidylcholine, DMPC.

3. Micellized Solutions of Surfactants

Figure 3 shows the structural formulas for several typical amphiphilic species that comprise important classes of surfactant. Each of these molecules prefers to satisfy the hydrophobic effect by means of a different local geometry (curvature). More explicitly, the SDS and CTAB form short and long cylindrical micelles, respectively. The CsPFO shows a strong preference for small disklike structures, and the phospholipids are well-known to organize spontaneously into bilayers and vesicles. We will return to these different preferences for local micellar curvature in sections 3.2 and 3.3. First, though, we simply note that the crucial common property of *all* amphiphilic species is that, as already mentioned in the Introduction, instead of undergoing a bulk phase separation at their solubility limit, they form finite aggregates—micelles—in order to satisfy the hydrophobic effect. In other words, what all these molecules have in common is a hermaphroditic or amphiphilic (Greek *amphi*, both; Greek *philos*, loving) nature, due to their highly hydrophobic "tails" and hydrophilic "heads". As also discussed in the first section, the basic phenomenon which must be accounted for is the change in average aggregation number which occurs as the concentration is raised, even in the dilute solution limit where micelles are not yet interacting with one another.

3.1. Dilute Solutions. Many statistical thermodynamic theories, of varying sophistication, have been developed to explain the variation with overall surfactant concentration of the average micellar size.[33−35] For purposes of illustration here, it is convenient to consider the case of surfactants which form rodlike micelles just above their cmc. Let E_N be the energy of a rodlike micelle consisting of N surfactants, and let x_N denote the mole fraction of such aggregates. Then the free energy of this dilute (noninteracting, ideal) solution of micelles can be written in the familiar form[35]

$$F = \sum_N x_N[E_N + \log(x_N)] \qquad (1)$$

Note that all energies here and henceforth are measured in units of k_BT. The equilibrium size distribution $\{x_N\}$ then follows from a minimization of F, subject to the mass conservation condition (fixed surfactant concentration) $\sum_N N x_N = X$, where X is the total mole fraction of surfactant in solution. The minimization yields

$$x_N = \exp[-(E_N - N\mu)] \qquad (2)$$

where μ is the Lagrange multiplier associated with the mass conservation constraint. It is straightforward to show that μ is

the chemical potential of surfactant molecules, which at equilibrium must be independent of whether they are monomers in solution or molecules in aggregates of arbitrary size N. Equation 2 can be written in a physically more suggestive form by setting μ equal, for example, to the chemical potential μ_1 of a monomer, using the ideal solution form $\mu_1 = \epsilon_1 + \log(x_1)$ and writing the energy E_N in the phenomenological form $E_N = N\epsilon_{rod} + E_{cap}$. Here ϵ_{rod} is the energy per molecule in the cylindrical ("body") portion of the micelle, and E_{cap} is the total excess energy of all the molecules in the two higher-curvature end caps of the rod (relative to their energy in the cylindrical body). In this way we obtain

$$x_n = x_1^N \exp[-(N\epsilon_{rod} + E_{cap} - N\epsilon_1)] \tag{3}$$

Note that eq 3 is simply an expression of the law of mass action applied to the molecular exchange equilibrium associated with aggregation of the surfactant molecules. More explicitly, noting that $N\epsilon_{rod} + E_{cap} - N\epsilon_1$ can be identified with the standard free energy change accompanying formation of the N-micelle from monomers, eq 3 assumes the more familiar form of the chemical equilibrium quotient for these "reactions"; $x_N/x_1^N = \exp(-\Delta G_N^\circ)$. The chemical species—"reactants and products"—here are the surfactant monomers and aggregates of different sizes N. From eq 3 we can immediately calculate many observable properties of the micellar solution, in particular the onset of spontaneous micellization at the cmc and the dependence of the average aggregation number on overall concentration, X. It is easy to show that

$$\text{cmc} \approx \exp[-(\epsilon_1 - \epsilon_{rod})] \tag{4}$$

and that the ("number") average micellar size is

$$\langle N \rangle = \sum_N N x_N \Big/ \sum_N x_N \approx [X \exp(E_{cap})]^{1/2} \tag{5}$$

The difference $(\epsilon_1 - \epsilon_{rod})$ is the transfer free energy associated with moving a surfactant molecule from its monomeric form in aqueous solution into its micellized state; it is typically on the order of 10−15 (in units of k_BT), thereby implying cmc mole fractions of 10^{-4}−10^{-5}. On the other hand, the only energy relevant to the size distribution well above the cmc is E_{cap}. This latter quantity, corresponding to the energy cost of moving enough molecules out of the cylindrical "body" to comprise the spherical "caps", is as large as 20. Accordingly, for mole fractions X on the order of 10^{-3}, say, $\langle N \rangle$ is as big as 10^{+3}; furthermore, this average aggregation number increases with concentration via the $^1/_2$ power, in agreement with experiment.[36]

In the above we have assumed that the preferred micellar shape is rodlike, i.e., that the optimum curvature for satisfying the hydrophobic effect is cylindrical, with higher energy caps (half-spherical, in this case) being necessary to "heal" the finite cylinder at its ends (shield the water from the hydrocarbon chains). Upon concentrating these systems, the entropy contributions log (x_N) in eq 1 become progressively less important than the energy terms E_N, and the latter must be minimized by ridding of caps, i.e., by rod length increasing. There are many examples of surfactants, however, which actually prefer the spherical geometry ($E_{cap} < 0$ for these systems) and whose micelles do *not* evolve into longer and longer rods upon increase in overall concentration. Rather, one simply sees more and more "minimum", globular/spherical micelles as surfactant molecules are added to the solution. Similarly, there are amphiphiles that choose at their solubility limit to satisfy the hydrophobic effect by organizing into bilayers (which in dilute solution close upon themselves as vesicles) with essentially zero curvature.

The issue of which local curvature is preferred just above the cmc, where interactions *between* micelles can be neglected, is closely related to the "dimensionality of growth", i.e., the dependence of the equilibrium size distribution on concentration according to whether one is dealing with prolate (rodlike, 1D) or oblate (disklike, 2D) aggregates.[37] A key difference between the rodlike and disklike micelles is that the size of the (spherical) caps of the rod is independent of micellar length, whereas the size of the (semitoroidal) rim of a disk increases with its diameter. This is essentially the same difference between the interfaces between up and down spin regions in the one- and two-dimensional Ising (or lattice gas) models, accounting for the absence of a phase transition in the former case.[10] One can, in fact, explicitly formulate the problem of micellar self-assembly equilibrium for rod and disk geometries, respectively, in terms of 1D and 2D Ising Hamiltonians, thereby explaining why cylinder size increases continuously with concentration while disks jump from small to infinite.[37] We return to this point in sections 3.5 and 5.1.

3.2. Intramicellar Molecules Packing. As emphasized already in the Introduction, it is not feasible at present to predict *a priori* which curvature (micellar geometry) will be preferred at the cmc for any given amphiphile in water. It is only possible to "explain" *a posteriori* with highly qualitative, descriptive arguments why, say, more or less positive curvature is expressed by the surfactants in their optimum micelles in dilute solution. For example, ionic amphiphiles whose headgroups bear a net charge and whose single hydrocarbon tails are relatively short will prefer to satisfy the hydrophobic effect with maximum positive curvature, i.e., they will form globular/spherical micelles; in that way the Coulomb-repelling heads are able to enjoy more lateral area than the tails, which can realize their need for conformational disorder without demanding too much lateral room. Alternatively, when the headgroup is neutral or zwitterionic, and there are *two* chains, both relatively *long*, then the surfactant will not be able to tolerate any positive curvature and will tend to organize as planar bilayers or even as "inverted" micelles (heads and water "inside", taking up less lateral space per molecule, and tails "outside", with more room). For intermediate situations, one expects cylindrical curvature to be optimum.

Early work through the 1970s assumed that the amphiphile heads were dominant over their tails in determining the preferred micellar geometry for a given surfactant in water. That is, the hydrophobic core consisting of the alkyl chains was taken to behave like a "liquid drop" of alkane, with complete neglect of how the chain free energies might depend on the size and curvature of the micelle: these geometric properties would simply adjust to optimize the headgroup area per molecule. More recent studies have established, however, that the free energy changes associated with the accompanying stretching and "splaying" of the alkyl tails are comparable to those of the heads and that chain packing effects must be taken into careful account.[38] Quite generally, the conclusions which emerge from these many theoretical and experimental investigations suggest a situation very different from that commonly pictured in textbooks. On one hand, there is considerable conformational order in the hydrocarbon chains: a plot of C−C bond orientational order vs carbon number shows a typical "plateau" for roughly the first half of the chain, even in the case of maximum positive curvature (i.e., the spherical micelles).[39] But the chains are definitely *not* fully stretched (all-trans) over all their length. For situations of positive curvature (spheres and cylinders, say)

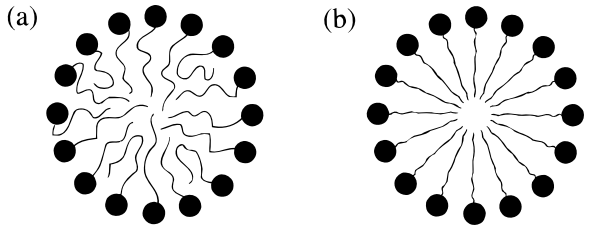

Figure 4. Schematic picture of chain packing in curved (spherical and cylindrical) micelles (a) as determined by theory[40−43] and experiment[44] and (b) as portrayed incorrectly in most textbooks.

there is simply no room for more than one or two chain ends in the center of the micelle! After all, the hydrophobic interior must be filled uniformly with methylene (CH_2) groups, in order that the density be essentially constant (and equal to the typical liquid alkane value): "nature abhors a vacuum" and does not tolerate large gradients that lead to much higher density. A schematic picture is shown in Figure 4a. Note that some of the chains are seen to wander on the surface before heading inside, while others are constrained to find their way back to the surface after first heading inward. Indeed, most of the volume of a small, positively curved region is necessarily associated with its surface! This is consistent with both the analytical[40−42] and simulation studies[43] of chain packing and with the observed fact[44] that the measured radial distribution of chain ends in spherical micelles shows a maximum at a position *halfway* to the center. Conversely, in bilayers, where there is *no* curvature, the chain ends are most likely to be found at the "center" (midplane). That is, here the chains *are* free to all head inward for their full length although there remains significant conformational disorder. Figure 4b shows the usual textbook drawing of chain packing in curved micelles, but it clearly makes no physical sense, since it necessarily involves an unrealistic buildup in local density at the micellar center.

3.3. Intermicellar Interactions. For the rest of this section we feature the very unique properties of concentrated micellar solutions, which result from their being colloidal suspensions of interacting particles *which do not maintain their integrity with regard to size and shape*. We have already seen in the above discussion how—even in dilute solution where the aggregates are essentially unaware of one another (no direct interactions between them)—the equilibrium size of micellar rods can increase with overall concentration. This is because of the competing requirements of "self-energy" (favoring longer rods and hence fewer high-energy caps) vs entropy of dispersion (favoring smaller aggregation numbers). At higher concentrations, where interactions *between* micelles begin to make an important contribution to the overall free energy of the solution, we must reexamine the possibilities and driving forces for change in micellar size. Again, it is simplest, for purposes of illustration, to consider rodlike aggregates. Furthermore, because the dominant interaction between micelles is most often repulsive, due to short-range steric forces, we shall confine our remarks to excluded-volume interactions. The leading corrections to ideal solution behavior (i.e., going beyond eq 1) can most easily be calculated by including the lowest order virial terms. In the case of steric forces (zero except for when the particles touch, whereupon they are infinite), the second- and third-virial coefficients have an especially physically pleasing, geometric interpretation: they simply correspond to the excluded volumes associated with pairs and triplets of particles. These in turn have been extensively treated for convex particles in general and for specific prolate, rodlike shapes in particular.[45] Furthermore, the virial series can be replaced by the much more quickly convergent "*y*-expansion"[46] and accurate free energies obtained for surfactant volume fractions on the order of several tenths. The technical details do not concern us here, but rather the conclusion that the packing entropy associated with a given volume fraction of colloidal rods is maximized by reorganizing them into a smaller number of larger rods. Recall that the entropy of dispersion favors small aggregation numbers, while the "self-energy" terms prefer larger ones (fewer caps). Accordingly, we find that the effect of (repulsive) intermicellar interactions is to shift the ideal solution balance *in the direction of larger micelles*.

When the surfactant concentration becomes still higher, we begin to have a problem finding room for the increasing number of larger rods. To pack them more efficiently, it becomes necessary for the micellized solution to develop long-range orientational order. Indeed, as discussed in section 2.2, Onsager has shown that, above a certain volume fraction, the free energy of a suspension of colloidal hard rods is minimized by an orientational distribution which is no longer uniform, but involves instead a preferred direction for the particle axes. So, micellar solutions of rods form nematic, liquid crystalline phases[47] for the same reasons as do "ordinary" colloidal suspensions of long, rigid macromolecules (e.g., TMV and PBLG). *But there is one fundamental difference*: in the case of micellar solutions there is—simultaneous with the onset of long-range orientational ordering—*an increase in the average size of the rods*. This is because each colloidal particle here is itself an aggregate comprised of a large number of individual molecules which are in exchange equilibrium with those in all other such particles. Accordingly, upon alignment, the system can organize itself into a smaller number of large particles, in order to decrease the loss of orientational entropy (as well as to further decrease their excluded volume).

Note that as rodlike micelles increase in size in order to pack more efficiently, the average curvature of micelles is decreased. This phenomenon turns out to be absolutely fundamental for understanding the general evolution of micellar structure and progression of phase transitions in concentrated surfactant solutions. It is related to the basic geometric fact that close-packing volume fractions increase as the curvature of colloidal particles *decreases*. Recall the well-known fact that the maximum volume fraction to which spheres can be packed is $\pi/\sqrt{18} = 0.74$ and that this requires hexagonal long-range order. On the other hand, if we reorganize the spheres into (infinitely) long cylinders and then align them and pack them hexagonally, the maximum volume fraction can be as large as $\pi/\sqrt{12} = 0.91$, the closest packing value for disks in a plane. Finally, if we reorganize the micelles instead into planar bilayers, we can pack them most efficiently of all; i.e., we need not "waste" any space, consistent with the fact that sheets can fill space perfectly up through volume fractions of unity. The key point is that, as micellar aggregates evolve from their most highly curved (spherical/globular) to least curved (planar bilayer) shapes, they present less excluded volume toward one another and pack more efficiently, thereby lowering the interaction free energy which becomes increasingly important at high concentrations. Of course, both the "self-energy" terms (involving local preference for a particular curvature) and the entropy of dispersion contributions *work against* this tendency to form larger, less-curved aggregates, but these single-particle free energy contributions eventually become overwhelmed at high enough volume fractions.

3.4. Ordered Phases and Defects. With the above qualitative arguments in mind, it is now straightforward to understand not only why micellar size increases with concentration in isotropic solutions, and why the nematic phase is reached, but

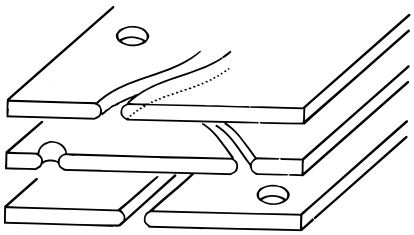

Figure 5. Schematic picture of "crack" and "hole" defects in the bilayers of high-concentration lamellar phases formed from surfactants which prefer to organize as curved micelles (cylinders and spheres) in dilute solution.

also why the nematic phase of rodlike micelles eventually must give way to a hexagonal phase of (essentially infinite) aligned cylinders. As the hexagonal phase is concentrated further, the average size of rods increases, and ultimately it is only a lamellar phase of stacked bilayers which allows the packing to be sufficiently efficient. But at this point it appears we have "squeezed" all local curvature out of the system! And recall that we have been discussing a surfactant solution which specifically prefers to satisfy the hydrophobic effect by means of cylindrical geometry. So, how can we insist on a lamellar phase of bilayer and also indulge the system in its local preference for cylindrical micellar curvature? The answer is that the bilayers are riddled with "cracks" which involve half-cylindrical "lips" to shield the water from the hydrocarbon chains; see Figure 5. These cracks are especially interesting defects because they involve a *negative* core energy; i.e., the local energy per molecule in a cylindrical lip is *lower* than that in the surrounding bilayer. But, of course, to create such a defect, one has to remove surfactant molecules from the bilayer and put them somewhere else, either crowding them elsewhere in the *same* bilayer or forming *new bilayers*. In the former case the bilayers thicken, and in the latter they become more numerous, leading in both instances to an increased repulsive interaction between bilayers. It is precisely this interaction between bilayers which keeps the defects from proliferating and destroying the lamellar phase; equivalently, it is this interaction which gave rise to the bilayers in the first place, to relieve the crowding of more curved structures (cylinders) in the hexagonal phase.

The scenario we have just recounted lies at the heart of a more quantitative theory which addresses the very different natures of lamellar phases of different classes of surfactant.[48] On one hand, we have the phospholipids, which like to satisfy the hydrophobic effect by forming bilayer structures at their solubility limit. For these systems, the lamellar phases which appear at high concentrations are of the "classical" kind, i.e., essentially perfect bilayers which admit a few defects but only at high enough temperature. On the other hand, we have the curvature-loving surfactants which prefer, say, to organize as cylindrical micelles at their cmc. These solutions are progressively forced to give up their local curvature as the volume fraction of surfactant is increased, following the sequence of structures and phases which we have outlined immediately above. The lamellar phases in these instances are characterized by a high density of defects which is very sensitive to the overall concentration because of the controlling influence of the interbilayer interactions. As the phase is concentrated, the curvature defects are "squeezed out", in order to minimize the defects of repulsions between the bilayers. Conversely, as the phase is diluted the local curvature defects proliferate, and the lamellar state gives way to the hexagonal phase of cylinders. Recent experimental work[49] has nicely confirmed this picture in the particular case of SDS/decanol solutions.

3.5. Ternary Solutions and Open Problems. *Ternary* systems, i.e., *two* amphiphilic species plus water, are of special interest because the composition—specifically, the relative number of each surfactant—can be used to "tune" the preferred local curvature. This effect is of most importance at low overall concentration, since the aggregates are essentially not interacting with each other. At high concentration we have seen, in the above discussion of binary systems, that the effect of intermicellar packing constraints is to favor the aggregates which have lower curvature. In the ternary cases, both composition *and* concentration play a role, either working in concert or at cross purposes. More explicitly, consider the example of a dilute solution of a phospholipid and of a surfactant which prefers cylindrical curvature. If the lipid is the dominant species, vesicles will be the major form of aggregate, each composed of mostly lipid with a little bit of surfactant dispersed uniformly throughout these closed bilayers. If, on the other hand, at fixed overall concentration of amphiphile, we begin to replace lipid by surfactant, there will be a transition from lipid-rich vesicles to surfactant-rich micelles (cylinders with small amounts of lipid).[50,51] This transformation will be discussed in more detail in section 5.4. If we had started instead with a pure lipid solution at *high* concentrations, we would have a classical lamellar phase; replacing lipid by surfactant at constant amphiphile volume fraction would then give rise to a lamellar-to-hexagonal transition.

In closing this section on micellar solutions, we mention several ongoing challenges which require concerted theoretical and experimental attention. First, very little work has been done on the problem of electrostatic effects in ionic surfactant systems. Again, the key new ingredient which distinguishes the micellar situation from that of the usual colloidal suspension is its self-assembly aspect. While much effort continues to be devoted to polyelectrolyte solutions, including phenomena as "simple" as the effect of counterion screening on the conformational properties of flexible chains,[52] comparable questions are only beginning to be addressed for charged micelles.[53] In the latter case, one would like to know, for example, whether the growth of rodlike aggregates discussed earlier in this section is enhanced or suppressed by electrostatic contributions and, furthermore, whether a change in shape from prolate to oblate might be driven by such effects. More generally, work needs to be done on establishing the physical bases for the appearance and stability of disklike micelles. It appears, for example, in the case of perfluorinated fatty acid salts that a transition from rods to disks is seen at low surfactant concentration and that in the presence of added salt it is possible to observe a demixing (upon lowering the temperature) of isotropic solutions of these micelles into dilute and concentrated phases of rods and disks, respectively.[54] These observations suggest new phase transition phenomena, again related to the unique coupling of the usual thermodynamic parameters (e.g., concentration) to micellar size and shape.

Finally, we mention that especially intriguing and novel structures are currently being reported in the experimental literature[55,56] and discussed in recent theoretical papers,[57−59] in particular the branched cylinders shown in Figure 6. Note that these branchings necessarily involve saddlelike curvature in regions of the junctions, i.e., in the "elbows" where one radius is positive (and of order the molecular length) while the other is negative and several times larger. Whereas such curvature is certainly less likely than those of the more familiar spherical

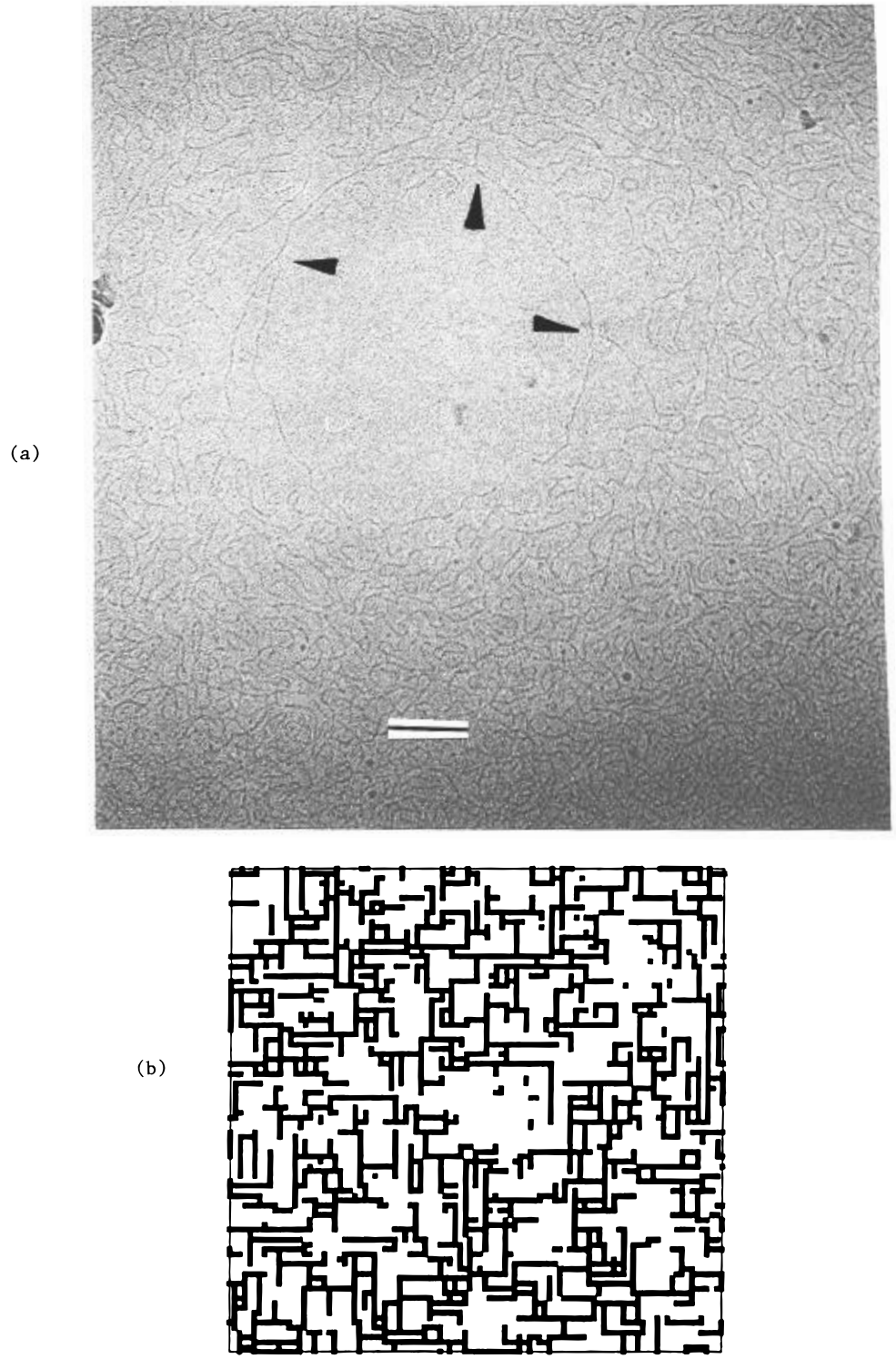

Figure 6. Branched linear micelles. (a) A cryo-TEM image of a dilute (2.2%) aqueous solution of a trimeric (triple-tailed) ionic surfactant.[55] Scale bar = 100 nm. The surfactants organize into flexible cylindrical (threadlike) micelles, revealing branched structures (junctions) indicated by arrows. Micrograph courtesy of Y. Talmon. (b) Equilibrium configuration from Monte Carlo simulation[57] of micellar systems in which surfactant prefers saddlelike geometry; see text.

or cylindrical geometries, say, there is no fundamental reason why it cannot be preferred by particular surfactants. Similarly, one must expect the outside or inside of a torus to be the preferred geometry for satisfying the hydrophobic effect in the case of still other amphiphiles. Accordingly, theories have been developed which explicitly incorporate all of these possibilities via a single, phenomenological Hamiltonian: it is of the Ising/lattice-gas type, but specifically includes three- and four-spin contributions which describe the dependence of micellar energy on local curvature.[37,57] Figure 6b shows results from Monte Carlo simulations for a system which prefers saddlelike geometry.

4. Interfacial Films and Microemulsions

4.1. What Is a Microemulsion? Everybody knows that oil and water do not mix with each other. This is because of the high energetic cost associated with replacing water−water and oil−oil contacts by water−oil contacts. The small entropic

contribution to the mixing free enrgy (less than k_BT per molecule) cannot make up for the high energetic penalty. This energetic penalty is also responsible for the high surface tension between bulk oil and water (≈30−50 dyn/cm) and for the sharpness of the interface between these liquids. Now, surfactant molecules, as their name indicates, are surface-active. They tend to adsorb at the water−oil interface, and when a sufficient amount of them is available, they create new low-tension interfaces separating mesoscopic domains of oil and water. The resulting mixtures, known as *microemulsions*,[60−69] can be *thermodynamically stable*. More commonly, when either the wrong kind or insufficient amounts of surfactant are used, the dispersions of oil in water or water in oil involve interfacial tensions which are too high to allow for thermodynamically stability. These systems, known simply as *emulsions*, degrade with time (sometimes in seconds, sometimes in months) into bulk phases of pure oil and pure water, with bits of surfactant dissolved preferentially in one or the other. On the other hand, "good" or "strong" surfactants form thermodynamically stable microemulsions, acting as mediators between water and oil and facilitating their mixing.

There are three basic types of microemulsions. In the case of oil-in-water (o/w) microemulsions, oil droplets of mesoscopic size (10−100 nm) are dispersed in water. The droplets are typically coated by a "positively" curved monolayer of surfactants, with their polar headgroups facing the continuous aqueous phase and their tails in contact with the oil. An o/w microemulsion can coexist with an "upper" bulk oil phase (Winsor I equilibrium[64,65]). The macroscopic surface tension between the microemulsion and oil phases is much lower than that between pure water and oil (say, 0.1 vs 50 dyn/cm). The above picture is reversed in the case of w/o microemulsions, where droplets of water, coated by a negatively curved surfactant monolayer, are dispersed in a continuous oil phase. A w/o microemulsion can coexist with an excess water ("lower") phase (Winsor II equilibrium). Again, the microscopic surface tension between these phases is very low. Under certain conditions a *three*-phase (Winsor III) equilibrium is possible. Here, a "middle" microemulsion phase, containing comparable amounts of water and oil, coexists with a lower aqueous phase and an upper oil phase. The middle phase is *bicontinuous*, consisting of two complementary interwoven labyrinths of oil and water, forming a spongelike structure[67−69] (Figure 7). The width of the continuous oil and water regions is typically on the order of 10 nm. The surfactant-saturated interfaces separating the oil and water regions fluctuate randomly in size and orientation, with the consequence that the bicontinuous phase is isotropic. All the macroscopic surface tensions in the three-phase system are *ultralow*, reaching about 10^{-2} dyn/cm.[64] Throughout the microemulsion phases the surfactant is the minority component present, typically in concentrations no larger than a few percent.

The possibility of mixing oil and water and the very low surface tensions in these systems are of great practical importance. For instance, emulsions enable solubilization of organic solutes in (the oil droplets of) aqueous solution, thus providing the basis for detergency. Similarly, the possibility of achieving extremely low interfacial tension is an essential requirement for tertiary oil recovery. In view of the many industrial applications of emulsions and the challenging thermodynamic, structural, and rheological properties of these complex systems, it is not surprising that many experimental and theoretical studies have focused on investigating their properties. Currently, fundamental research activity in this area is tapering off from its fever pitch of this past decade. But many challenging problems remain, including the effects of flow on the relative stabilities

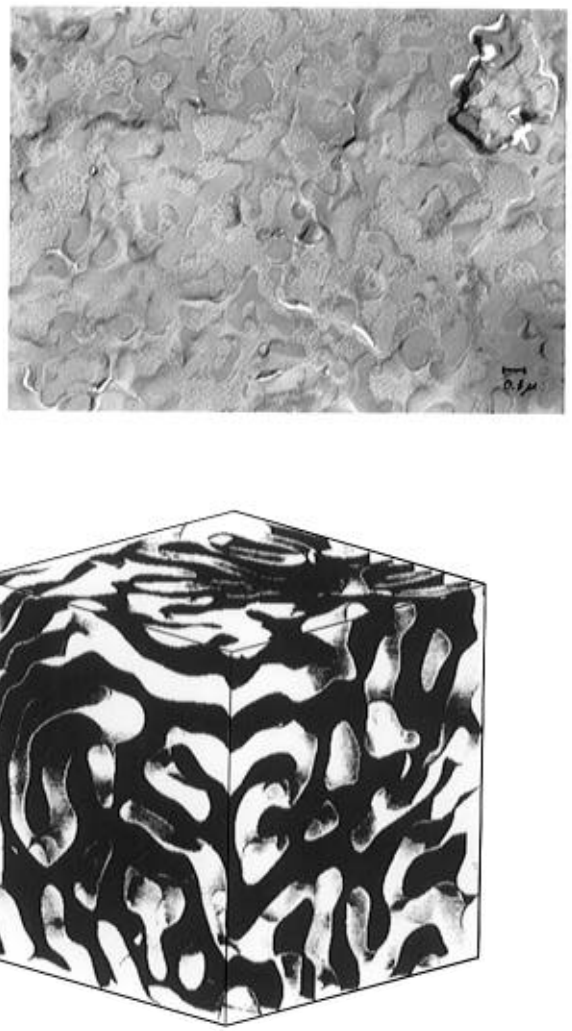

Figure 7. (a) Freeze-fracture electron microscopy image of a bicontinuous microemulsion. The mixture consists of comparable amounts of water and oil (octane) and 7 wt % of the nonionic surfactant $C_{12}E_5$. The fracture face of water (amorphously frozen) appears gray, while the oil regions are textured. Micrograph courtesy of R. Strey. (b) A computer simulation[69] image of a spongelike bicontinuous microemulsion. Flexible, wrinkled surfactant films separate the water and oil domains. Courtesy of P. Pieruschka.

of lamellar, bicontinuous, and droplet phases; the control of "shape transitions" and anisotropy in the structural evolution of microemulsion "drops"; and their direct observation and visualization via, for example, newly developed confocal optical imaging[14] and cryogenic vitrification electron microscopy.[5,6]

In the rest of this section we shall describe the basic principles governing the thermodynamic behavior of microemulsion, synthesizing the recent ideas and results of many researchers in this field. In particular, we shall try to explain, qualitatively, which factors determine the structure of microemulsions and to understand the origin of the low interfacial tensions associated with their appearance.

Due to their amphiphilic nature, surfactant molecules tend to adsorb at water−oil interfaces, their heads "anchored" in water and their tails "dissolved" in the oil. The adsorbed surfactants replace part of the direct water−oil contacts by energetically more favorable water−headgroup and tail−oil contacts. Furthermore, the adsorbed monolayer behaves as a two-dimensional fluid which, for entropic reasons, tends to expand. This tendency results in a lateral pressure Π which reduces the effective surface tension between the oil and water phases from its "bare" value γ_0 to $\gamma = \gamma_0 - \Pi$.[61,64]

When a small amount of surfactants is added to a system containing water and oil, some of them adsorb at the interface and some dissolve into one or both of the bulk phases. In general, the surfactants strongly prefer one bulk phase over another. Suppose they are only soluble in water. As long as the concentration of surfactants in water is below their cmc, they will partition between the interface and (as monomers) in the bulk phase, as dictated by the equality of their chemical potentials in the two environments. The three-dimensional water phase is preferred, entropically, over the interface which, in turn, is preferred on energetic grounds. If the surfactants in solution tend to form micelles, then, above the cmc, not only the monomer concentration in solution stays constant but also the surfactant concentration at the interface. All newly added surfactants will participate in micelle formation, and the interfacial monolayer reaches its saturation concentration.

The formation of micelles is a consequence of the fact that the constituent surfactants are "curvature loving". When the micelles appear in the aqueous phase, this means that interheadgroup repulsions are much stronger than intertail repulsions. In the opposite case "inverted" micelles are formed in the oil phase. Neither kind of surfactants is suitable for the formation of microemulsions. Rather, a basic characteristic of the interfacial surfactant films in microemulsions, especially in bicontinuous phases, is their *low spontaneous curvature*.[70,71] By low curvature we mean that the radius of curvature is considerably larger than the thickness of the surfactant film which, typically, is on the order of 1 nm. Good emulsifying surfactants should prefer to form monolayers of low curvature; i.e., they should be those whose headgroup and tail repulsions nearly balance each other. In mixtures involving single tail ionic surfactants this condition can be reached either by adding salt, which partly screens the electrostatic repulsion between the charged headgroups, or by adding cosurfactants. Generally both salt and cosurfactant are added to the mixture. The cosurfactant, usually a short-chain alcohol, is incorporated into the monolayer between the charged surfactants, thus acting as a spacer, reducing electrostatic repulsion. The short cosurfactant chains also reduce intertail repulsions, thus lowering the bending rigidity of the interfacial film, a property of crucial importance for decreasing the macroscopic interfacial tension in microemulsion systems, as will be explained below. In systems based on nonionic surfactants, such as C_nE_m's $[(CH_3(CH_2)_{n-1}(OCH_2CH_2)_mOH)]$, the spontaneous curvature and bending rigidity are controlled by temperature and by the lengths of the polar (m) and hydrophobic (n) moieties of the amphiphile.[63]

Efficient emulsifying surfactants should also be "strong amphiphiles"; that is, they should prefer the oil−water interface over dissolving in one or both of the bulk phases.[63,67] In this case, once the original water−oil interface is saturated, then all added surfactants participate in creating new interfaces, resulting in the formation of microemulsions. The surfactants composing the saturated interfaces are densely packed. The average cross-sectional area per hydrocarbon chain in these films, $a_0 \approx 30$ Å^2, is larger than the minimal area ($\approx$20 Å^2) of a fully stretched ("all-trans") chain but small enough to ensure that the chains are in close contact with each other, forming a rather compact liquid film. Changing the average area per surfactant in the monolayer (a) by more than a few percent involves much larger free energy cost than bending the film. Therefore, in the following discussion we shall assume that $a = a_0$ in all water−oil interfaces regardless of their curvature.

The free energy of an interfacial surfactant film is the (surface) integral of the local free energy; the latter is a function of the local area per molecule, a, and the two principal curvatures $c_1 = 1/R_1$ and $c_2 = 1/R_2$; R_1 and R_2 are the local radii of curvature. (Recall our convention that $R > 0$ if the interface is convex toward the water.) Following our assumption that all interfaces are saturated and inextensible ($a = a_0$), the local free energy density (i.e., the free energy per unit area) $f = f(c_1,c_2)$ is only a function of curvature. A general expression for f for small curvatures ($c < 1/l$, where l is the thickness of the surfactant film) is[70−72]

$$f = {}^1/_2K(c_1 + c_2 - 2c_e)^2 + {}^1/_2\bar{K}(c_1 - c_2)^2 \qquad (6)$$

with K and $\bar{K}$ denoting two independent curvature elasticity moduli, and c_e is the spontaneous curvature of the surfactant film. The free energy is a minimum when $c_1 = c_2 = c_e$. The value of c_e is governed by the balance of the moments of forces arising from headgroup repulsion, surface tension, and tail−tail repulsion. (Stronger headgroup repulsions imply $c_e > 0$, and conversely.) The elastic moduli depend sensitively on the chemical composition of the surfactant film, the chain lengths of the constituent surfactants, and the average cross-sectional area per chain a_0 (see section 5.3). In general, $K \approx 10k_BT$ for pure surfactant films. By mixing the surfactant with a comparable amount of cosurfactant, the bending rigidity K is largely reduced, typically to $K \approx 1k_BT$ at room temperature.[73−75]

4.2. The Origin of Ultralow Interfacial Tensions. Now, how are the bending rigidity and the spontaneous curvature related to the structure of microemulsions and to the low macroscopic surface tensions characterizing these systems?

Consider a mixture containing comparable amounts of oil and water and a small amount of surfactant, that is, $\phi_o \approx \phi_w \gg \phi_s$ with ϕ_o denoting the volume fraction of oil, etc. Suppose for concreteness that $c_e > 0$, and ignore the concentration of monomeric surfactant in the bulk phases. A small fraction of the surfactants will adsorb at and saturate the oil−water interface. The rest will be used to coat oil-in-water microemulsion droplets. Ignoring size and shape fluctuations, these droplets can be treated as spherical, with radius $R = R_e = 1/c_e$. The volume fraction of oil in the o/w microemulsion phase, $\phi_{o/w}$, is fixed by ϕ_s and by the ratio of the film volume, $4\pi R_e^2 l$, to oil volume $4\pi R_e^3/3$: $\phi_{o/w} \simeq (R_e/3l)\phi_s = \phi_s/(3lc_e)$. If ϕ_s is too small, then (even though $R_e \gg l$) only part of the oil will be solubilized in water; the rest will be expelled as a pure bulk phase coexisting with the o/w microemulsion ("emulsification failure").[71] What then is the interfacial tension between these two phases?

The curvature of the surfactant monolayer at the oil−microemulsion interface, $c_1 = c_2 = 0$, is not the optimal one. To increase the interfacial area and yet keep the interface saturated, it is necessary to unfold (optimally curved) microemulsion monolayers. This involves an entropic loss which we shall ignore here and an energy penalty which is easily evaluated using eq 6. Explicitly, the curvature free energy cost for an interface area δA is $\delta F = \delta A[f(c_1{=}c_2{=}0) - f(c_1{=}c_2{=}c_0)] = \delta A 2Kc_e^2 = \delta A 2K/R_e^2$. The effective surface tension $\gamma = \delta F/\delta A$ is thus

$$\gamma = 2K/R_e^2 \qquad (7)$$

showing that both small bending rigidity and small spontaneous curvature help in lowering γ.[61] As a numerical estimate, suppose $K \approx 1k_BT$ and $R_e \approx 10$ nm, implying $\gamma \approx 2 \times 10^{-2} k_BT/(\text{nm})^2 \approx 0.1$ dyn/cm, as compared to $\gamma \approx 50$ dyn/cm for the bare water−oil surface tension.

Upon increasing the surfactant concentration, it is possible to solubilize *all* of the oil in the water phase, obtaining a single microemulsion phase. This happens when $\phi_s \simeq (3l/R_e)\phi_0$.

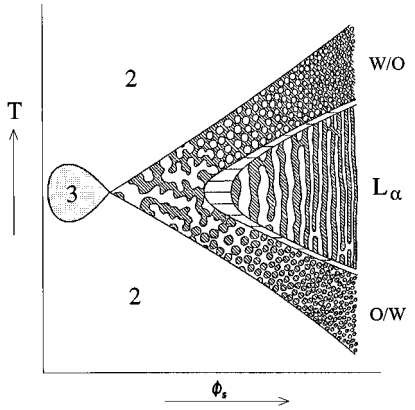

Figure 8. Schematic illustration[68] of the structures and phase behavior of a microemulsion consisting of comparable amounts of oil and water and varying amounts (ϕ_s) of a nonionic surfactant. The digits 2 and 3 denote two- and three-phase regions. Note the bicontinuous structures at the origin of the "fishtail", and the lamellar phase (L_α) appearing as ϕ_s increases.

Beyond this value the surface/volume ratio of the oil globules must increase. Indeed, both experiment and theory reveal the appearance of cylindrical oil globules and eventually the formation of lamellar phases.[71]

4.3. Isotropic Bicontinuous vs Lamellar Phases. Returning to eq 7, it appears that as $R_e \rightarrow \infty$ the surface tension should vanish. Recall, however, that we ignored the entropic contribution to γ. Note also that when $R_e \rightarrow \infty$ the minimal curvature energy corresponds to flat surfactant interfaces or, in other words, to a lamellar phase consisting of alternating layers of water and oil, separated by surfactant films. Indeed, lamellar phases are observed, but only at relatively high values of ϕ_s. When ϕ_s is low (and $R_e \rightarrow \infty$), the more stable microemulsion phase is the bicontinuous one. Since this phase is isotropic and consists of randomly oriented interfaces, the origin of its low free energy must be entropic.

As noted earlier, the bicontinuous phase is a spongelike structure composed of tortuous oil and water domains, separated by "crumpled surfactant sheets". These surfactant sheets are wrinkled—bend freely—on all length scales larger than ξ_K, the persistence length of the monolayer. Qualitatively, we expect that ξ_K increases with the bending rigidity of the film. Indeed, it can be shown that ξ_K increases exponentially with K/k_BT.[61] For $K/k_BT \approx 1$ one finds $\xi_K \approx 10$ nm, which is actually the typical length scale of microemulsion domains.

Consider again a water−oil−surfactant mixture with $\phi_0 \approx \phi_w \approx {}^1/_2 \gg \phi_s$, now with $c_e \approx 0$. Suppose for a moment that all surfactant molecules are organized in parallel flat sheets separating oil and water layers. The average distance between adjacent surfactant monolayers would then be $d = l\phi_0/\phi_s \approx l/2\phi_s$, with l the thickness of the monolayer. If $d > \xi_K$, there is no reason for the surfactant sheets to stay flat. They can wrinkle (undulate) nearly freely, thus increasing their entropy, without "bumping" into each other. The opposite behavior is expected when $\xi_K > d$, i.e., when $\phi_s > (l/\xi_K)$, explaining the higher stability of the lamellar phase at sufficiently large surfactant volume fractions.[61,66,71]

Figure 8 shows a schematic phase diagram of a microemulsion mixture, indicating the one-, two-, and three-phase regions in a system containing equal amounts of oil and water and a varying amount of surfactant, ϕ_s. The shape of the three-phase region in this $T-\phi_s$ diagram, corresponding to a system based on nonionic surfactants, is known as the "fish".[63,67,68] Similar behavior is observed in systems containing ionic surfactants (and cosurfactants), but with the temperature axis replaced by the salinity S of the aqueous phase. By changing T in nonionic systems or S in ionic systems, one tunes the spontaneous curvature of the surfactant film. The values of T or S "along the backbone" of the fish correspond, roughly, to $c_e = 0$. At the three-phase region a bicontinuous middle phase coexists with oil-rich and water-rich phases. The upper and lower phases disappear at the tail of the fish. Increasing ϕ_s beyond this point leads, eventually, to the transition from the isotropic (spongelike bicontinuous) phase to the lamellar phase.

According to our very qualitative analysis above, the surfactant concentration at the three-phase region is such that $\phi_s < l/\xi_K$. The question then arises: why does the system separate into three coexisting phases rather than stay as one homogeneous random phase? There are a number of ingenious theories which account for this behavior,[60−62,66,67] but for the purpose of the present discussion it suffices to treat this issue on a very qualitative level.

Suppose we regard the isotropic, bicontinuous phase as a random arrangement of water and oil regions, say cubes of side length λ, arranged on a cubic lattice. A surfactant layer of area λ^2 and volume $\lambda^2 l$ separates neighboring water-filled and oil-filled cubes of the lattice. The number of cubes per unit volume is $1/\lambda^3$. The probability that a given cube is filled with oil is ϕ_o, and the probability that any of its nearest-neighbor cubes will be filled with water is ϕ_w. Hence, the average number of oil−water pairs is proportional to $\phi_o\phi_w$. The interface between such pairs, of area λ^2, is covered by surfactants, implying that the average volume fraction of surfactant, per cube, is $\lambda^2\phi_o\phi_w$, and hence $\phi_s \sim 1/\lambda$. Thus, regardless how small is ϕ_s, it is always possible to arrange the system with the cubes large enough (large λ) to cover all water−oil interfaces with surfactants. However, the "mixing entropy" of water and oil on the lattice, per unit volume, scales with the number of cubes, namely, $S_{mix} = (k_B/\lambda^3)[\phi_o \ln \phi_o + \phi_w \ln \phi_w]$.[66] Thus, the smaller is λ, the larger is S_{mix}, and it is not surprising that the system prefers to stay random on the smallest length scale possible, expelling the excess water and oil into separate phases. But λ cannot be made too small because once it is comparable to ξ_K, the bending energy penalty will become appreciable. Hence, the middle phase will stay random, on a length scale λ which is of the order of ξ_K. The surface tension between the bicontinuous phase and the oil or water phases is expected to be extremely low. The major effect of increasing the surface area between these phases is to transfer a certain amount of a randomly fluctuating surfactant interface from the bulk (continuous) phase into the interfacial region. These fluctuations are slightly damped at the interface, but the free energy cost is minimal.

5. Bilayers

The most abundant and important aggregation geometry of amphiphiles in nature is the bilayer, i.e., two monolayers combined tail to tail. A lipid bilayer provides the structural basis for all cell (plasma) membranes and surrounds (or constitutes) the various intracellular organelles such as mitochondria, the Golgi apparatus, lysosomes, and the cell nucleus.[76,77] Biological membranes are composed of various kinds of amphiphiles, mostly phospholipid molecules, and in many cases also cholesterol and glycolipids. Integrated within the plasma membrane or adsorbed on its outer or inner surfaces are many proteins, fulfilling biochemical functions and providing communication channels between the cell and its environment. The lipid−protein membrane of living cells is coupled to two macromolecular networks. The inner surface is connected to a rubberlike cytoskeleton, consisting of a flexible protein (spec-

trin−actin) network which imparts mechanical stability and flexibility to the cell membrane. The outside surface is coupled to the glycocalix, a carbohydrate network responsible for cell−cell recognition and adhesion.[34,76,77]

The lipid bilayer of biomembranes is a strong elastic film. It can be slightly stretched or compressed and, more easily, undergo curvature deformations. The lipids can diffuse laterally within the membrane, which can thus be regarded as a 2D fluid. The conformational freedom of the lipid chains is responsible for the membrane elasticity, which plays a crucial part in the transport of proteins, lipids, neurotransmitters, and other biomolecules across the bilayer membranes between different cell organelles or between different cells. This delivery process involves membrane invagination followed by *vesicle* budding.[76−78] The vesicle, a self-closed (nearly spherical) bilayer, encapsulates biomolecules and carries them to another cell or organelle where, via *fusion* with its membrane, it releases its contents into the target compartment. Thus, biological cells contain many vesicles (whose sizes range typically between 250 nm and 1 μm) which serve as delivery vehicles for biomaterials from one compartment to another. Imitating nature, synthetic vesicles are often used in pharmacology and medicine as transport vehicles of drugs, enzymes, DNA, and other molecules into living cells.[79]

The composition of the lipid mixture and the protein content of cell membranes are highly specific to the function of the cell. Most cells do not function if the delicate balance of lipids and proteins is perturbed. Nevertheless, considerable insights into many physicochemical properties of biological membranes can be gained from experimental and theoretical studies of simplified model membranes, e.g., unilamellar vesicles composed of only a few lipid components. For example, synthetic model vesicles exhibit similar shape (curvature) fluctuations to those observed in the "flickering phenomena" of red blood cells.[77,78] The rigidifying effect of cholesterol on lipid membranes is also observed in model lipid−cholesterol vesicles.[80] Similarly, considerable information on the adhesion and fusion of cells is obtained from using a variety of force measurements on model vesicles and membranes.[81]

Lipid molecules are not the only amphiphiles which organize into bilayers. Most amphiphiles including both ionic and nonionic surfactants form, within a wide range of conditions, a variety of lamellar, vesicular, and sometimes more exotic (e.g., spongelike) phases of bilayers.[82−85] Many of these systems are of practical importance, posing also a host of challenging theoretical questions concerning their phase behavior. Considering the enormous importance of bilayers, we devote this section to a brief outline of the principles governing their formation, growth, stability, and flexibility.

5.1. Bilayer Growth. Phospholipids in water self-assemble into extended bilayer sheets because they cannot comfortably pack into micelles. They would if they could, because micelles are smaller objects and are therefore preferred on entropic grounds. However, because of their bulky (double-chained) hydrophobic tails and relatively small polar heads, the packing of phospholipids into positively curved spherical or cylindrical micelles involves an exorbitant energetic price. Accordingly, most lipids self-assemble into planar bilayers and in some instances even organize in "inverted" (cubic and/or hexagonal) phases as is indeed observed in certain systems.[86]

Two monolayers combine into a bilayer in order to avoid exposing their hydrophobic interfaces to water. However, since the monolayer's spontaneous curvature is never exactly zero, and since the curvatures of the two apposed monolayers in vesicles are necessarily of opposite signs, at least one of them is not optimally curved. Thus, bilayer formation generally involves a certain curvature "frustration" energy cost. It is easily shown that the frustration energy is minimal when the bilayer is planar, i.e., when the two principal curvatures of the bilayer (measured at its midplane) are identically zero, $c_1 = c_2 = 0$. In other words, the spontaneous curvature of the *bilayer* is zero, $c_e^{(b)} \equiv 0$. More precisely, $c_e^{(b)} = 0$ for a symmetric bilayer, that is, a bilayer composed of two identical monolayers. This result follows from the fact that the curvature (free) energy of a symmetric bilayer must satisfy $F(c_1,c_2) = F(-c_1,-c_2)$. Using eq 6 for the curvature energy per unit area, but now in a bilayer rather than in a monolayer, it follows immediately that $c_e^{(b)} \equiv 0$. Equation 6 can also be used to estimate the curvature energy associated with forming a planar bilayer from two *monolayers* characterized by a nonzero spontaneous curvature, $c_e \neq 0$. Setting $c_1 = c_2 = 0$ in this equation, we find that the average bilayer curvature energy density is $f = (K/2)c_e^2$. Typically, for double-tailed lipid bilayers $K \approx 10k_BT$ at room temperature. But the (monolayer) spontaneous curvatures of bilayer-forming amphiphiles are small, $|c_e| \ll 1/l \approx (1/15)$ Å^{-1}. Thus, even for a rather high spontaneous curvature, say $c_e \approx (1/100)$ Å^{-1}, we find that the curvature frustration energy, $f \approx 10^{-3}k_BT$/Å^2, is quite small. By small, we mean that it is smaller, in fact negligible, compared to the energetic cost (per unit area) associated with exposing the hydrophobic tails of one, even optimally bent, monolayer to water. This latter quantity is on the order of the hydrocarbon−water interfacial tension, $\gamma \approx 50$ dyn/cm $\approx 0.1k_BT$/Å^2, much higher than the curvature energy penalty estimated above.

The three canonical aggregation geometries of amphiphiles in water—the spherical micelle, the cylindrical micelle, and the bilayer—involve different "growth dimensionalities". By "growth" we mean here the increase in average aggregation number *upon increase in surfactant concentration*. Spherical micelles cannot grow because the radius of each sphere cannot exceed the molecular length, and hence their growth dimensionality is $D = 0$. Cylindrical micelles can grow linearly and thus correspond to $D = 1$. As already noted in section 3, the growth of linear micelles is analogous to the condensation of a 1D lattice gas or to domain growth in a 1D Ising spin system. In these 1D systems the entropy loss involved in the association of small aggregates (domains) into fewer larger ones is not compensated for by the corresponding (edge) energy gain. Consequently, these systems do not exhibit a condensation phase transition, and the growth of aggregates (or spin domains) is continuous. On the other hand, bilayers are 2D systems, which can grow along their two lateral dimensions. In 2D systems a first-order condensation transition is possible below a certain critical temperature, T_c, inversely proportional to the strength of the attractive interparticle potential. In the case of bilayers, the "particles" are *pieces* of bilayer which can be attracted to one another because of the opportunity for thereby lowering their "rim" energy. More explicitly, a *disk*- or *ribbon*like portion of bilayer in aqueous solution necessarily involves a curved cylindrical rim, in order to shield the water from its constituent hydrophobic tails. To the extent that its molecules prefer to pack *without* this (cylindrical) curvature, there is an energy cost arising from the presence of rims. Accordingly, as two bilayer portions associate into one, curved-rim molecules are converted into planar bilayer. Using, say, the curvature-energy lattice-gas model[37,57] mentioned at the end of section 3, it follows that a 2D condensation transition to infinite bilayer will occur whenever the rim energy is large enough. Otherwise, disklike micelles will dominate.

5.2. Vesicles *vs* Lamellar Phases. The driving force for bilayer growth, as in any other nucleation−condensation phenomena, can be attributed to the tendency of a growing condensed phase aggregate to minimize its unfavorable edge energy. (In 2D systems the fraction of "high-energy" edge molecules decreases as $N^{-1/2}$ where N is the total number of molecules in the aggregate.) However, since amphiphilic bilayers are flexible, they have another option for getting rid of their edges: they can close upon themselves to form *vesicles*.

Vesicle formation involves a certain curvature energy penalty since the optimal bilayer configuration is planar. On the other hand, vesicles carry some translational entropy, and their equilibrium size distribution will thus be determined by the balance between entropic and energetic contributions to the free energy of the system. Theoretically, it is quite simple to derive the expressions governing the size distribution of (spherical) vesicles in dilute aqueous solutions. On the other hand, the experimental determination of the equilibrium size distribution is considerably more difficult since, at least in most lipid systems, vesicle formation is not a spontaneous process, because (monomeric) lipids are essentially insoluble in water. Thus, before discussing the size distribution of lipid vesicles, let us briefly digress to add a few comments about their preparation.

When phospholipids are dispersed in water they form closed multibilayer aggregates, often called *liposomes* or multilamellar vesicles (MLV). Considerable input of mechanical or chemical energy is generally required to unfold the liposomes into single bilayer vesicles.[87] Among the common mechanical methods are sonication and high-pressure extrusion through filters of small pore size. The size of the vesicles can be controlled by the intensity and period of sonication or by the size of the micropores. These methods enable the formation of unilamellar vesicles with radii ranging from ≈10 nm to ≈10 μm. Another method for preparing vesicles is to dissolve the lipids in a volatile organic solvent which is then dispersed in water. Upon evaporation of the organic solvent the lipids self-assemble into vesicles. Still another "chemical" technique is to "solubilize" the MLV's into micelles by the addition of detergents. The detergent is a single-tailed curvature loving surfactant which, when alone in water, self-assembles into micelles. The detergent incorporates into the lyposome bilayers, first mixing with the lipids, but above a certain (saturation) concentration the bilayer is destabilized and the vesicle decomposes into mixed lipid−surfactant micelles. The surfactant is then removed by dialysis, i.e., by adding excess water, and the lipids reorganize into unilamellar vesicles. This last process is often used in the reconstitution of lipid−protein membranes. The inverse process, the vesicle−micelle transition, plays a major role in *in vivo* fat metabolism.[76,88]

The size distributions of the vesicles formed by the methods mentioned above are strongly influenced by kinetic considerations and by the mode of preparation. In most cases the vesicles eventually aggregate or reorganize into multilamellar liposomes. Thus, it is not at all clear if and when the size distribution of the vesicles corresponds to true equilibrium. Nevertheless, let us try to determine by simple thermodynamic considerations what the size distribution should look like. Assuming that the vesicle density in solution is small, the size distribution will be determined by the interplay between the translational (mixing) entropy and the self- (curvature) energy of the vesicle. Recalling that the spontaneous curvature of the bilayer is zero, we find from eq 6 that the curvature energy per unit area in a spherical vesicle of radius R is $f = 2K/R^2$, with K denoting the bending rigidity of the bilayer. It should be noted that this expression is valid for large vesicles, so that R is much larger than the bilayer thickness (≈2l), and we can neglect differences in the curvatures and aggregation numbers between the inner and outer monolayers. The total curvature energy is then $E_N = 8\pi K$, i.e., E_N is independent of R. Note, however, that the free energy per molecule $8\pi K/N$, where $N = 2(4\pi R^2)/a_0$, is of course size dependent. Thus, for a solution with a given amphiphile concentration the curvature energy per molecule decreases as the size of the vesicles increases.

The self-assembly equations used in section 3 to calculate the size distribution of rodlike micelles can also be used for vesicles. After some harmless approximations, we find[7,89] for the average aggregation number

$$\langle N \rangle = \sqrt{X}\exp(4\pi K) \tag{8}$$

The average vesicle radius is $\langle R \rangle \approx [\langle N \rangle a_0/8\pi]^{1/2} \sim X^{1/4}$, with a_0 denoting the average cross-sectional area per molecule (typically, for double-tailed lipids $a_0 \approx 60-70$ Å^2). The bending rigidities of lipid bilayers, K, are generally ≈10k_BT or even larger. From eq 8 it follows that even for very dilute lipid solutions, e.g., $X = 10^{-6}$, the average aggregation number is enormous. More detailed analyses of the vesicle size distribution (e.g., taking into account vesicle shape fluctuations[89]) would not change this conclusion. It thus appears that an equilibrium distribution of finite size vesicles is only possible if K is small (as may be the case in mixed bilayers, see below). As a concrete example we estimate the value of K corresponding to an average vesicle radius of, say, $\langle R \rangle = 1000$ Å when the total lipid concentration is $X = 10^{-6}$: $K \approx 1.5k_BT$. This analysis is valid as long as the average distance between vesicles is large compared to their diameter. When the vesicles begin to crowd in space, their translational entropy is essentially lost, and a phase transition into a lamellar (L_α) phase of extended, and more comfortably packed, bilayers will take place.

Phospholipids are not the only amphiphiles which organize into bilayers, and the vesicle (sometimes denoted as L_4) and lamellar (L_α) phases are not the only structures that bilayers can form.[82] Aqueous solutions of surfactants of the kind used in microemulsions, such as the nonionic amphiphile $C_{12}E_5$, exhibit a host of isotropic and ordered phases.[85] At $t \approx 60$ °C and surfactant volume fraction $\phi_s \geq 0.013$, the system forms an ordered (smectic-like) L_α phase, with repeat distance decreasing linearly with ϕ_s. Below $\phi_s = 0.013$ a new phase appears, coexisting with the L_α phase. Small-angle neutron scattering (SANS) and conductivity measurements reveal quite clearly that the new phase (called L_3) is isotropic and *spongelike*. It resembles the bicontinuous phase of microemulsions, except that now a crumpled bilayer membrane (rather than a monolayer) separates disconnected water regions (rather than water and oil). Sponge phases are also observed in aqueous solutions of ionic surfactants upon addition of cosurfactants such as short chain alcohols. Again, as mentioned in the previous section, the added alcohol serves to lower the spontaneous curvature of the film and to reduce its bending rigidity.

5.3. Molecular Models. In this article we have repeatedly mentioned that the addition of a cosurfactant, i.e., a short-chain amphiphile into a film (monolayer or bilayer) of long-chain amphiphiles, lowers the bending rigidity of the film. Surfactant−cosurfactant films are just one example of mixed systems which are of great interest in various contexts (e.g., the vesicle−micelle transition in mixed lipid−surfactant systems). The properties of pure and mixed films depend of course on the packing characteristics of the constituent molecules, and it is important to describe briefly some of the microscopic aspects of amphiphile packing in bilayers and their influence on membrane elasticity.

The hydrocarbon chains constituting the hydrophobic core of lipid bilayers are densely packed, with the monomer (segment) density being similar to that in bulk liquid hydrocarbons of similar chain length.[7,35] Thus, the hydrophobic core is liquid-like or, more precisely, liquid-crystalline-like, because the amphiphile chains are highly stretched along the membrane normal. The average end-to-end distance of the hydrocarbon chains in the bilayer, l, is considerably larger than the average end-to-end distance, l_0, in a bulk hydrocarbon liquid. More precisely, $l = d/2$ where d is the thickness of the bilayer hydrophobic core. The average cross-sectional area per chain in the membrane is $a = v/l$, where v is the chain volume. Typically, $a \approx 30 - 35$ Å^2 in bilayers as compared to the smallest possible area per chain, $a_m \approx 20$ Å^2, corresponding to a fully stretched ("all-trans" in the case of an alkyl) chain. Since $a > a_m$, the chains possess considerable conformational freedom, although less than in isotropic liquids. (Below a certain temperature, the lipid chains in bilayers undergo a phase transition into a crystalline phase, where all chains are fully stretched and $a = a_m$.[91] However, we are interested only in the fluid, "liquid crystalline" phase of the bilayer.)

Because of their restricted conformational freedom, the chains in the membranes tend to expand (i.e., to increase a), thereby exerting a lateral pressure π_t on their neighbors. The polar headgroups also repel each other, due to electrostatic and/or excluded-volume interactions. These two repulsive forces which tend to increase a are balanced by the hydrocarbon−water interfacial tension γ, which tends to minimize the hydrocarbon−water contact area and hence to lower a. The balance of these forces determines the equilibrium area per chain, a_0.

Experimentally it is known that the bending rigidity, K, increases with increasing chain length, n, and decreases with increasing area per molecule, a. It is also known that the bending rigidity of a surfactant film is lowered substantially upon the incorporation of shorter chain amphiphiles into this film.[73] Several detailed theoretical studies have addressed these issues;[74,75] more interestingly still, straightforward scaling arguments applied to a simple chain compression model[74,75] also account nicely for the relevant experimental findings. If headgroup repulsions dominate, for example, it can be shown for a series of amphiphiles with the same headgroup that K increases with chain length (carbon number, n) as n^3. When chain repulsions dominate, on the other hand, K varies more moderately with n, $K \sim n^{4/9}$. The compression model can be extended to mixed bilayers (or monolayers) composed, say, of long- and short-chain amphiphiles. The extension is not trivial, and the resulting dependence of K on the mole fraction of, say, the short chains is nonlinear.[75] (K decays rapidly to its short chain limit, reaching this value already when the mole fraction of these chains is ~0.5.) Yet, qualitatively it is clear that adding short chains to a film composed of longer chains amounts to a reduction of the "effective" chain length of the mixture. Also, the short chains can be regarded as spacers separating the longer chains (which provide the main contribution to K), thus effectively increasing the average cross-sectional area of these chains. Both effects, the lowering of the average n and the increase of the effective a, result in a lower value of K.

5.4. Mixed Systems. By Gibbs' phase rule, the number of thermodynamic degrees of freedom of a macroscopic system increases by one whenever a new molecular species is added. This larger number of composition degrees of freedom in multicomponent systems is generally accompanied by richer and more complex phase behaviors. This trend is even more dramatically manifested in complex fluid mixtures of self-assembling amphiphiles. Structural transformations and phase transitions in these systems can appear in different forms and on different length scales. Some phase transitions take place within one aggregate, others involve a transition from one aggregation geometry to another but within the same macroscopic phase, and certain transitions are accompanied by macroscopic phase separation. Quite often, a phase transition takes place simultaneously on all length scales. We illuminate these points by some specific examples.

Phase transitions within a single aggregate are often observed in mixed lipid bilayers. As in ordinary 3D liquid or solid solutions, binary lipid membranes exhibit a "demixing" transition, resulting in the coexistence of two domains, characterized by different lipid compositions. Such transitions can be explained in terms of approximate (e.g., regular solution) theories, with the critical temperature T_c inversely proportional to $w = (w_{AA} + w_{BB})/2 - w_{AB}$ ($w > 0$), where w_{AB} is the pair potential between lipids A and B, etc.[91] Less ordinary interaction potentials may be responsible for phase transitions in certain lipid−protein membranes. Integral (hydrophobic) proteins are generally rigid and thus reduce considerably the chain conformational freedom of the surrounding lipid molecules. This perturbation results in an elastic deformation, and hence free energy increase, of the local lipid environment which is proportional to the surface area of the embedded protein.[92−95] Consequently, the membrane proteins tend to aggregate in order to lower the number of conformationally perturbed lipid chains. Here, again, below a certain critical temperature, the *lipid-mediated* (elastic) protein−protein interactions induce a protein condensation phase transition.

The demixing of components in lamellar or vesicular phases of bilayers is often coupled to changes in the packing curvature, sometimes even inducing a major structural transition. Consider, for example, a mixed vesicle composed of two kinds of amphiphiles (whose pure monolayers are) characterized by different spontaneous curvatures, e.g., one moderately positive and the other moderately negative. If the mixed bilayer is symmetric, i.e., the compositions of its two constituent monolayers are identical, then its spontaneous curvature is zero and, consequently, vesicle formation involves a finite free energy penalty. This curvature energy can be lowered by adjusting the compositions of the outer (positively curved) and inner (negatively curved) monolayers, so that the spontaneous curvature of the outer monolayer is slightly positive and of the inner slightly negative. This gain in curvature energy is, however, opposed by the loss of mixing entropy. Theoretical calculations indicate that, in general, if the mixing is ideal this process is unfavorable and the planar (symmetric) bilayer state is more stable than the curved (demixed) vesicular geometry, explaining why in most systems vesicle formation is not a spontaneous process.[75,96,97] An interesting exception has recently been demonstrated in aqueous solutions of single-tailed ionic amphiphile mixtures, in which the headgroups of the two amphiphilic components are oppositely charged.[98] It was found that when these amphiphiles are dispersed in water, they aggregate spontaneously to form thermodynamically stable mixed micelles.

Other forms of curvature−composition coupling are possible when curvature-loving (micelle-forming) surfactants are added to an aqueous solution of lipid vesicles. At low concentration of surfactant, encouraged by the mixing entropy, these molecules will incorporate into vesicles. Within the bilayer, the mixing is not necessarily ideal. There is strong experimental evidence that some lipid vesicles become leaky once they incorporate a sufficient amount of surfactant, suggesting that the curvature-loving surfactants aggregate and form micropores within the

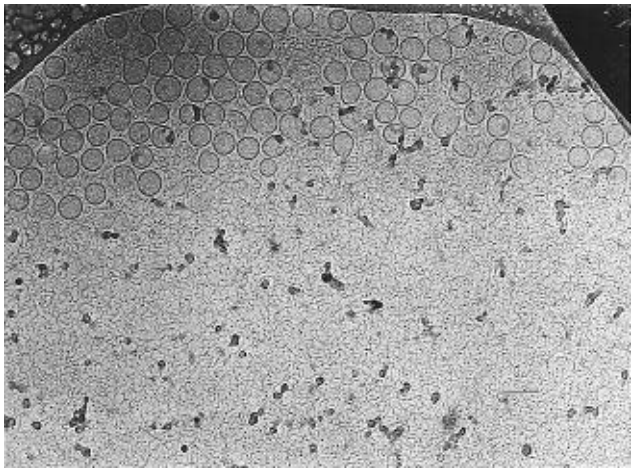

Figure 9. The vesicle−micelle transition. A cryo-TEM image of a lecithin ("lipid")−sodium cholate ("detergent") mixture, illustrating the coexistence between mixed vesicles and threadlike micelles.[102] Scale bar = 100 nm. Note the existence of partially solubilized vesicles. The crowding of the vesicles in one region of space is due to the confining effect of the thin cryo-TEM sample; there is no macroscopic phase separation in this system. Micrograph courtesy of Y. Talmon.

bilayer.[99,100] One can imagine that the surfactants pack at the semitoroidal lips of these pores.

The vesicle−micelle transition is probably the best-documented phenomenon demonstrating a compositionally induced structural transformation.[50,51,101−104] As mentioned briefly earlier, a lipid vesicle can only accommodate a certain amount of curvature-loving surfactants in its bilayer. Beyond a critical mole fraction of surfactants in the bilayer ($x_s \approx 0.5$ in lecithin−bile salt mixture), the vesicle is no longer stable; the bilayer is disrupted and breaks into micelles. Not surprisingly, the mole fraction of surfactants is larger in the highly curved micelles ($x_s \approx 0.75$ in the above system). Upon adding more surfactant to the solution, additional vesicles are decomposed until they all disappear. Before this happens, vesicles and micelles coexist in solution, as is clearly demonstrated in Figure 9. The vesicle-to-micelle transformation is thus a truly first-order phase transformation. The two phases, which differ in both their composition and structure, are mesoscopic rather than macroscopic and are embedded in the same macroscopic phase (the aqueous solution).

6. New Materials

6.1. Metal Nanocrystals. The first example we will feature is that of nanocrystal dispersions, in particular the stabilization of nanoscale crystallites of noble metals in organic solvents. We are all aware of the past decade's tremendous level of research activity on nanoparticle syntheses, especially in the case of semiconductor materials; this work has been addressed directly in the article by Alivisatos elsewhere in the current volume. What is perhaps less well-known is the fact that these particles can be prepared not only via nucleation and arrested growth processes but also as equilibrium products, so that thermodynamic control of their size becomes a real possibility. To appreciate the basic physical−chemical principles involved, it is instructive to recall briefly the situation mentioned in our earlier section on microemulsions.

Very crudely speaking, what accounts for the thermodynamic stability of a dispersion of, say, water drops in oil is the lowering of the water/oil interfacial tension to values which are orders of magnitude smaller than the "bare" water/oil value. Otherwise, the energy cost associated with drop surface is intolerable, and the dispersed system will spontaneously get rid of its interfacial area by reverting to two bulk phases. Let γ denote as before the interfacial energy per unit area of a drop. Then, for drops of size R, the surface energy cost per drop (dropping all numerical factors) is simply γR^2. This energy must be offset by the lowering of the free energy due to the entropy of dispersion, which latter—on a "per drop basis"—is of order k_BT. Thus, γR^2 must be smaller than k_bT. This (admittedly oversimplified) argument allows us to estimate how small the interfacial tension must be in order for the dispersion of water in oil to be thermodynamically stable. More explicitly, since $R \approx 100$ Å $= R_{min}$ is a reasonable lower bound to the size of a drop (significantly smaller R would no longer allow us to speak of a drop!), we find immediately that γ must not exceed k_BT/R_{min}^2, or 10^{-4} k_BT/Å^2. Without any surfactant, the tension is as high as 50 dyn/cm or about $(1/10)k_BT$/Å^2. Thus, the role of added amphiphile, as has been long known and widely appreciated (see our discussion in section 4), is to lower the water/oil interfacial tension by orders of magnitude.

Now, how do we exploit the analogy between the above fluid/fluid phenomenon and the situation of nano*crystal* dispersions? The particluar system we consider here is that of gold nanoparticles in simple organic solvents, because recent results reported in the literature[105−107] illustrate our arguments quite thoroughly and because of the intimate connection to self-assembled monolayers (SAM's) on gold, which are discussed at length by Whitesides elsewhere in this volume. The choice of surfactant for the gold/organic solvent systems is a natural one, since so much work has already been done on the strength of the gold−*thiol* bond, specifically in the context of SAM's of long-chain alkanethiols on gold. Not only is the bond between thiol and gold strong enough to give rise to the high densities of self-assembled thiols, adsorbed onto gold from organic solutions, but it *also* does the job of essentially ridding the surface tension of gold in the solvent! In this way, a dispersion of gold particles in, say, hexane or toluene, becomes thermodynamically stable, for the same reasons as outlined just above for the more familiar water-in-oil microemulsions. Consequently, we can exploit the fact that the nanoparticles are equilibrium products (of the reaction to be described in a moment) and thereby control their size by simply adjusting the relative numbers of surfactant and gold in solution.

The most recent synthesis of gold nanocrystals soluble in organic solvent proceeds as follows:[105] gold (tetrachloride) salts are reduced at room temperature in aqueous solution by boron tetrahydride salts, in the presence of dodecanethiol, and transferred to toluene via tetraoctylammonium ions. The resulting nanocrystals of gold are shown to be "capped" with the dodecanethiol and to have a 2 nm metal core diameter. Changing nothing but the amount of thiol, it was then shown[106] that the average size of nanocrystal products could by controlled directly by the composition of the reagents. Specifically, varying the gold/thiol ratio from 1:1 to 6:1 resulted in the average diameter increasing from 2 to over 10 nm. The basic idea is that most of the long-chain thiol will bond to the gold surface (thereby lowering its energy enough to essentially remove the interfacial tension) and that the *amount* of surface for a given quantity of gold, i.e., the surface-to-volume ratio of the particles, will simply be determined by the amount of thiol relative to gold. Since each particle diameter corresponds to a different surface-to-volume ratio, the nanocrystal size will be essentially fixed by the gold/thiol composition, as is indeed seen in the experiments, including results for other noble (e.g., silver) and transition (platinum, palladium) metals.[106] These developments constitute an exciting example of the rational control of nanoparticle size.

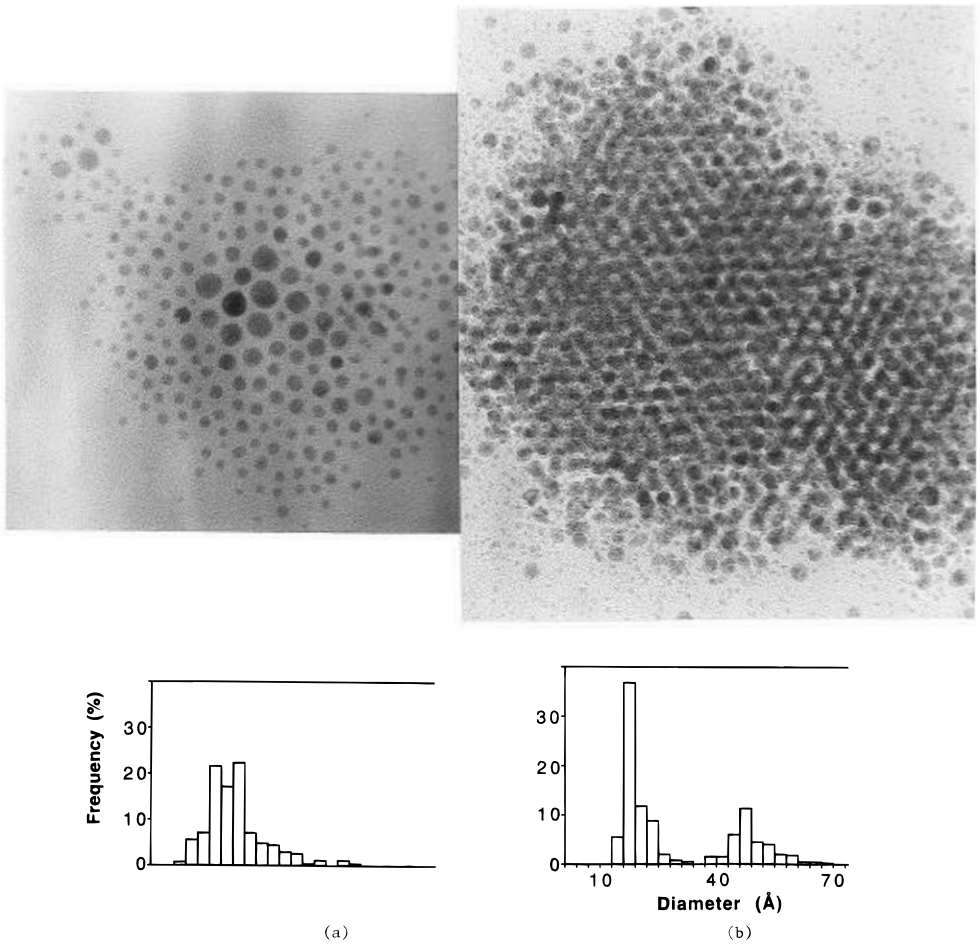

Figure 10. (a) TEM picture of alkanethiol functionalized gold nanocrystals which spontaneously crystallize in 2D with radial size segregation, from an evaporating drop of hexane on an amorphous carbon substrate;[107] the corresponding size distribution is shown directly below. (b) TEM image of a 3D hcp opal formed upon evaporation of a hexane solution (with the size distribution shown below) on a water surface. Micrographs courtesy of J. R. Heath.

6.2. Plastic Spheres. The analogy with fluid−fluid microemulsions discussed above for the syntheses of metal nanocrystals has also been beautifully exploited in the instance of polymer lattices. Emulsion[108] and microemulsion[109] polymerization techniques have long been applied for preparing narrow size distributions (in the submicron range) of spherical plastic particles. The latter case is especially relevant to our present discussion, because *composition* is again used in the *thermodynamic* control of *size*, just as in the metal nanocrystal situation. For example, polystyrene lattices with radii of tens of nanometers have been prepared[110] in microemulsions formed by dispersion of styrene in water, with their precise size (surface-to-volume ratio!) determined by the mole ratio of ionic surfactant (C_{16} alkylammonium chloride, say) to styrene; polydispersity indices are as small as a few percent. These particles, once polymerized by addition of cross-linker and initiator, can also be made to swell homogeneously in the presence of further monomers, thereby providing a means for construction of latex particles with more complex architectures, e.g., interpenetrating microgels or hollow spheres, etc. Functionalization of the particle surface (via addition, say, of water-soluble methacrylate *co*monomers, or the use of block copolymers as cosurfactants) during the polymerization step is also of considerable scientific and practical interest.[110]

It is also possible to control the incorporation of electronically and optically interesting materials into submicron colloidal particles. A particularly compelling example of such nanocomposites is that of 50−300 nm monodisperse silica spheres which contain semiconductor quantum dots (e.g., CdS)! Again, as in the cases discussed immediately above for *organic*, polymer particles, comparably small *in*organic spheres can also be prepared via microemulsion methods. The silica colloids are produced, for example, from controlled hydrolysis of tetraethyl orthosilicate in water "nanodroplets", with CdS dots incorporated by the simultaneous coprecipitation of cadmium nitrate and ammonium sulfide. Furthermore, the *morphology* of the CdS can be "engineered" to be a dispersion—*within* the silica particles—of 2−3 nm dots or large inclusions, surface caps, central core, or interleaved shells.[111] These various CdS structures can also be etched out, to give silica particles with corresponding *void* morphologies, with obvious applications as mesoporous/nanoporous materials.

6.3. Array Formation. For all of the nanoparticle syntheses described above, many intriguing possibilities for new materials arise from consideration of their subsequent self-assembly *on a larger length scale* to form mesoscopic crystals or opals. Figure 10a shows an electron micrograph prepared[107] by evaporating a drop of gold nanocrystals in hexane on an amorphous carbon-coated TEM grid; the corresponding particle size distribution is shown directly below. At the center of the micrograph we see a close-packed domain of the largest (5−6 nm) particles, with smaller ones "wetting"/ordering about this cluster as they extend in the outward radial direction to still smaller sizes. Note that the separation between nearest-neighbor particles is independent of the particular gold core diameters involved and corresponds approximately to twice the alkanethiol film thickness. By evaporating similar gold-in-hexane dispersions as Langmuir films on water, it is possible to form *three-*

dimensional (hexagonal-close-packed) opals, consisting of thousands of gold nanoparticles, with the largest ones again surrounded by the smaller ones as one moves out progressively from the center; see Figure 10b. The exceptional aspect of these results is that long-range ordering (opal formation) of the particles is not frustrated by the considerable polydispersity in their distribution of sizes and furthermore that the radial segregation serves to sort out the different sizes. These phenomena are consequences of the fact that the ordering is driven by macroscopic dispersional (van der Waals) attractions whose strength is an increasing function of particle diameter.

The formation of ordered arrays is more commonly driven by electrostatic repulsions between colloidal particles. A well-studied case is that of poly(methyl methacrylate) (PMMA) spheres, which can be prepared as highly monodisperse suspensions with radii in the 0.1 μm range and with high surface charge (from, say, copolymerization with ionic surfactant) and hence strong interparticle repulsions: in low-ionic-strength water these systems "self-assemble" into bcc and fcc crystals, with lattice constants in the near-IR and visible regions. Accordingly, these systems provide natural opportunities for novel optical applications. For example, the particles can be refractive index matched at normal light intensities, but designed with large enough optical nonlinearity—via incorporation of either CdS quantum dots or (covalently linked) absorbing, nonfluorescent dye molecules—so that they Bragg diffract incident light when its power exceeds a certain threshold.[112]

It is interesting to contrast the behavior outlined above with the case of aqueous solutions of somewhat larger gold particles which have proved so useful in studying kinetic aggregation processes and the fractal structures which result from them.[113] Here the particles are formed via reduction of gold salts by trisodium citrate and are highly charged because of the surface-adsorbed citrate ions. Aggregation is initiated by the addition of pyridine which successively displaces the charged citrate, leading to strong attractions between the particles. Beautiful fractal structures are observed[113] as a consequence of this irreversible sticking, allowing in particular for incisive tests of simple models of diffusion-limited aggregation (DLA). In the case of the opal formation discussed in the preceding paragraph, the fundamental difference is that the gold cores of the thiol-capped particles never get closer to one another than several nanometers (surface-to-surface distance), and hence the dispersional attractions never exceed thermal energies by too much.

6.4. Foams, Gels, and Mesoporous Materials. In this final section we make just a few remarks about novel "soft-condensed-matter" materials, in particular liquid-based foams, reversible gels, and inorganic/organic mesoporous media systems.

By stirring up water in air, in the presence of the right mixture of surfactants, foams—dense, random dispersions of gas bubbles packed into a relatively small volume of liquid—are commonly prepared. These systems are remarkable insofar as they can resist static shear like a solid, flow and deform as a liquid (under large enough applied stress), and be compressed like ideal gases! While not usually thought of as materials, they do nevertheless have many unique applications which derive from these elastic and rheological properties, as well as from their dramatically low density and high internal surface area. From a practical point of view, they are fundamentally important because of their ubiquity in industrial processing, throughout businesses as diverse as food, cosmetic, detergent, mining, petroleum, pulp and paper, paint and coating, textile, leather, polymer, and waste and water remediation. And, as complex fluids, foams are challenging because of their being organized on several different length scales, ranging from the microscopic (surfactant structure in the single-molecule-thick interfacial films between water and air) through the mesoscopic (thickness of water layers and sizes of gas bubbles) to the macroscopic. Nevertheless, it is only recently that systematic attempts have been made to interrelate the physics of these diverse length scales and to apply modern experimental and theoretical ideas to their investigation. For slowly draining foams it is now possible to measure flow properties in a rheometer and simultaneously monitor "bubble-hopping" rearrangements via multiple-scattering, diffusing-wave spectroscopy.[114] The observed distribution of times *between* these events is quite narrow, consistent with current models of 3D bubble-scale foam rheology[115] but at odds with predictions from *two*-dimensional theories.[116]

Another class of "soft" material which is attracting much interest is that of reversible gels, such as those formed in aqueous solution via the micellization of hydrophobic side chains in water-soluble polymers. A much-studied example involves the radical copolymerization of acrylamide with alkyl acrylates or alkyl acrylamides containing large hydrophobic groups (such as perfluorinated alkanes).[117] By varying the alkyl comonomer species (including the length of various spacer groups within it), its concentration relative to the dominant acrylamide, and the overall copolymer weight percent in aqueous solution, samples with a wide range of viscosities can be prepared. Especially intriguing is the nonmonotonic effect of adding monomeric surfactants: low concentrations lead to a dramatic increase in viscosity, while higher amounts lead to a maximum and subsequent *de*crease. The initial increase is believed to arise from micellization of the hydrophobic side chains with one another, leading to cross-linking of the polymer backbone, facilitated by monomeric surfactant from solution. At higher concentrations, however, the surfactant progressively *displaces* the side chains from these micelles, thereby undoing the cross-links. The optimization of systems of this kind obviously needs to be pursued, with the goal of controlling "on and off" mechanisms for reversible gels.

A final example of the synergism between complex fluid phenomena and new frontiers in materials science is provided by recent breakthroughs in the syntheses of mesoporous media.[118] Here one sees an especially rich interplay between inorganic and organic self-assembly. The basic idea is to interrelate the structures (in, e.g., the cubic, hexagonal, and lamellar phases discussed earlier in section 3) of micellized solutions of ionic surfactants to the organization of condensed ("polymerized") silicates. The resulting nanometer-scale voids provide (upon burning off of all the organic material) high surface area for catalysis applications and high selectivity for molecular sieves. The "problem", however, is that the micellar phases do *not* serve simply as "templates" for the polymerization of silicate into zeolite structures; e.g., one does not observe the same sizes and shapes of voids that were present as micelles in the precursor surfactant-in-water system. Instead, because of strong interactions and competing hydration effects among the silicate ions (and their various oligomeric forms) and the surfactant ions, there arise new preferences for micellar curvature and long-range ordering in the mixed systems. Nevertheless, with the concerted application of powerful tools such as small-angle neutron scattering, high-resolution solid-state NMR spectroscopies, and freeze-fracture electron micrographs, clever strategies have been developed for controlling structures and properties of these important classes of inorganic/organic mesophases.

Acknowledgment. We are pleased to thank our many students and co-workers for their extremely valuable and

enjoyable contributions over the past dozen years to our understanding and progress in this field. For financial support we acknowledge grants from the United States National Science Foundation (W.M.G.), the Israel Science Foundation (A.B.S.), the Minerva Foundation, Munich (A.B.S.), and the US/Israel Binational Science Foundation (A.B.S. and W.M.G.).

References and Notes

(1) Debye, P. *Ann. N.Y. Acad. Sci.* **1949**, *51*, 575.
(2) Berne, B. J.; Pecora, R. *Dynamic Light Scattering*; Wiley: New York, 1976.
(3) Jacrot, B. *Rep. Prog. Phys.* **1976**, *39*, 911. Cabane, B.; Duplessix, R.; Zemb, T. *J. Phys.* **1985**, *46*, 2161.
(4) Seelig, J.; Niederberger, W. *Biochemistry* **1974**, *13*, 1585.
(5) Bellare, J. R.; Davis, H. T.; Scriven, L. E.; Talmon, Y. *J. Electron Microsc. Tech.* **1988**, *10*, 87.
(6) Zasadzinski, J. A. N.; Bailey, S. M. *J. Electron Microsc. Tech.* **1989**, *13*, 309.
(7) Israelachvili, J. N. *Intermolecular and Surface Forces*, 2nd ed.; Academic Press: New York, 1992.
(8) See, for example: Smit, B.; Hilbers, P. A. J.; Esselink, K.; Rupert, L. A.; van Os, N. M.; Schlijper, N. M. *J. Phys. Chem.* **1991**, *95*, 6361.
(9) Larson, R. G. *J. Chem. Phys.* **1992**, *96*, 7904.
(10) See, for example: Plischke, M.; Bergersen, B. *Equilibrium Statistical Physics*, 2nd ed.; World Scientific: Singapore, 1994. Stanley, H. E. *Introduction to Phase Transitions and Critical Phenomena*; Oxford University Press: New York 1971.
(11) Rowlinson, J. S.; Widom, B. *Molecular Theory of Capillarity*; Oxford University Press: New York, 1989; Chapter 3.
(12) Friedman, H. L. *A Course in Statistical Mechanics*; Prentice-Hall: Englewood Cliffs, NJ, 1985; Chapter 9.
(13) Pusey, P. N.; Poon, W. C. K.; Ilett, S. M.; Bartlett, P. *J. Phys.: Condens. Matter* **1994**, *6*, A29 and references to earlier work cited therein.
(14) van Blaaderen, A.; Wiltzius, P. *Science (Washington, D.C.)* **1995**, *270*, 1177. White, W. R.; Wiltzius, P. *Phys. Rev. Lett.* **1995**, *75*, 3012.
(15) Alder, B. J.; Wainwright, T. E. *J. Chem. Phys.* **1957**, *27*, 1208. Hoover, W. G.; Ree, F. H. *J. Chem. Phys.* **1968**, *49*, 3609.
(16) Woodcock, L. V. *Ann. N.Y. Acad. Sci.* **1981**, *37*, 274.
(17) Sanders, J. V. *Philos. Mag.* **1980**, *A42*, 705.
(18) Xu, H.; Baus, M. *J. Phys.: Condens. Matter* **1992**, *4*, 663. Edlridge, M. D.; Madden, P. A.; Frenkel, D. *Mol. Phys.* **1993**, *79*, 105.
(19) Asakura, S.; Oosawa, F. *J. Chem. Phys.* **1954**, *22*, 1255; *J. Polym. Sci.* **1958**, *33*, 183.
(20) Note that when the big particles are so large that "there is no place to hide", the smaller ones *do* end up being confined and the effective interaction is *repulsive*; this is in fact the origin of the classic repulsion between charged surfaces in aqueous solution whose counterions are trapped between them.
(21) Bibette, J.; Roux, D.; Nallet, F. *Phys. Rev. Lett.* **1990**, *65*, 2470.
(22) Onsager, L. *Ann. N.Y. Acad. Sci.* **1949**, *51*, 627.
(23) Fraden, S.; et al. *J. Phys.* **1985**, *46 (C3)*, 85; *Phys. Rev. Lett.* **1989**, *63*, 2068.
(24) Russo, P. S.; Miller, W. G. *Macromolecules* **1983**, *16*, 1690.
(25) Brian, A. A.; Frisch, H. L.; Lerman, L. S. *Biopolymers* **1981**, *20*, 1305.
(26) Bunning, P. A.; Philipse, A. P.; Lekkerkerker, H. N. W. *Langmuir* **1994**, *10*, 2106.
(27) Wen, X.; Meyer, R. B.; Caspar, D. L. D. *Phys. Rev. Lett.* **1989**, *63*, 2760.
(28) (a) Stroobants, A.; Lekkerkerker, N.; Frenkel, D. *Phys. Rev.* **1987**, *A36*, 2929. (b) Mulder, B. *Phys. Rev.* **1987**, *A35*, 3095. (c) Wen, X.; Meyer, R. B. *Phys. Rev. Lett.* **1987**, *59*, 1325. (d) Somoza, A. M.; Tarazona, P. *Phys. Rev.* **1988**, *61*, 2566. (e) Poniewierski, A.; Holyst, R. *Phys. Rev.* **1988**, *61*, 2461. (f) Taylor, M. P.; Hentschke, R.; Herzfeld, J. *Phys. Rev. Lett.* **1989**, *62*, 800.
(29) Grosberg, A. Yu; Kuznetsov, D. V. *Macromolecules* **1992**, *25*, 1991 and references therein.
(30) See, for example: Darnell, J.; Lodish, H.; Baltimore, D. *Molecular Cell Biology*; Scientific American Books: 1990.
(31) Bloomfield, V. A. *Biopolymers* **1991**, *31*, 1471 and references cited therein.
(32) Ubbink, J.; Odijk, T. *Biophys. J.* **1995**, *68*, 54. Vasilevskaya, V. V.; Khokhlov, A. R.; Matsuzawa, Y.; Yoshikawa, K. *J. Chem. Phys.* **1995**, *105*, 6595.
(33) Tanford, C. *The Hydrophobic Effect*, 2nd ed.; Wiley: New York, 1980.
(34) Israelachvili, J. N.; Mitchell, D. J.; Ninham, B. W. *J. Chem. Soc., Faraday Trans. 1* **1976**, *72*, 1525.
(35) Gelbart, W. M.; Ben-Shaul, A.; Roux, D., Eds. *Micelles, Membranes, Microemulsions and Monolayers*; Springer: Berlin, 1994.
(36) See, for example: Mazer, N. A.; Benedek, G. B.; Carey, M. C. *J. Phys. Chem.* **1976**, *80*, 1075. Porte, G. Chapter 2 in ref 35.
(37) Granek, R.; Gelbart, W. M.; Bohbot, Y.; Ben-Shaul, A. *J. Chem. Phys.* **1994**, *101*, 4331.
(38) See Ben-Shaul, A.; Gelbart, W. M. Chapter 1 in ref 35.
(39) Charvolin, J. *J. Chim. Phys.* **1983**, *80*, 15.
(40) Dill, K. A.; Flory, P. *J. Proc. Natl. Acad. Sci. U.S.A.* **1981**, *78*, 676.
(41) Gruen, D. W. R. *J. Phys. Chem.* **1985**, *89*, 146.
(42) Ben-Shaul, A.; Szleifer, I.; Gelbart, W. M. *J. Chem. Phys.* **1985**, *83*, 3597. Szleifer, I.; Ben-Shaul, A.; Gelbart, W. M. *J. Chem. Phys.* **1985**, *83*, 3612; **1986**, *85*, 5345; **1987**, *86*, 7094.
(43) Haile, J. M.; O'Connell, J. P. *J. Phys. Chem.* **1986**, *90*, 1875. Jonsson, B.; Edholm, O.; Teleman, O. *J. Chem. Phys.* **1986**, *85*, 2259. Watanabe, K.; Ferrario, M.; Klein, M. L. *J. Phys. Chem.* **1990**, *94*, 2624.
(44) Bendedouch, D.; Chen, S.-H.; Kohler, W. C. *J. Phys. Chem.* **1983**, *87*, 153.
(45) Tjipto-Margo, B.; Evans, G. T. *J. Chem. Phys.* **1990**, *93*, 4254 and references therein.
(46) Barboy, B.; Gelbart, W. M. *J. Chem. Phys.* **1979**, *71*, 3053; *J. Stat. Phys.* **1980**, *22*, 709. Mulder, B. M.; Frenkel, D. *Mol. Phys.* **1985**, *55*, 1193.
(47) See: Boden, N. Chapter 3 in ref 35.
(48) Bagdassarian, C. K.; Roux, D.; Ben-Shaul, A.; Gelbart, W. M. *J. Chem. Phys.* **1991**, *94*, 3030.
(49) Quist, P. O.; Fontell, K.; Halle, B. *Liq. Cryst.* **1994**, *16*, 235.
(50) Vinson, P. K.; Talmon, Y.; Walter, W. *Biophys. J.* **1989**, *56*, 669. Ollivon, M.; Eidelman, O.; Blumenthal, R.; Walter, A. *Biochemistry* **1988**, *27*, 1695. Almog, S.; Litman, B. J.; Wimley, W.; Cohen, J.; Wachtel, E. J.; Barenholz, Y.; Ben-Shaul, A.; Lichtenberg, D. *Biochemistry* **1990**, *29*, 4582.
(51) Andelman, D.; Kozlov, M. M.; Helfrich, W. *Europhys. Lett.* **1994**, *25*, 231. Fattal, D. R.; Andelman, D.; Ben-Shaul, A. *Langmuir* **1995**, *11*, 1154.
(52) de Gennes, P.-G. *Scaling Concepts in Polymer Physics*, Cornell University Press: Ithaca, NY, 1979. Khokhlov, A. R.; Khachaturian, K. A. *Polymer* **1982**, *23*, 1742. Borue, V. Yu.; Erukhimovich, I. Ya. *Macromolecules* **1988**, *21*, 3240.
(53) Odijk, T. *J. Phys. Chem.* **1989**, *93*, 3888; *J. Chem. Phys.* **1990**, *93*, 5172; *Physica* **1991**, *A176*, 201. Safran, S. A.; Pincus, P. A.; Cates, M. E.; MacKintosh, F. C. *J. Phys.* **1990**, *51*, 503; *Europhys. Lett.* **1990**, *12*, 697. Halle, B.; Landgren, M.; Jonsson, B. *J. Phys.* **1988**, *49*, 1235.
(54) Boden, N.; Brandao, M. Private communication.
(55) Danino, D.; Talmon, Y.; Levy, H.; Beinert, G.; Zana, R. *Science (Washington, D.C.)* **1995**, *269*, 1420.
(56) Khatory, A.; Kern, F.; Lequeux, F.; Appell, J.; Porte, G.; Morie, N.; Ott, A.; Orbach, W. *Langmuir* **1993**, *9*, 933. Khatory, A.; Lequeux, F.; Kern, F.; Candau, J. *Langmuir* **1993**, *9*, 1456.
(57) Bohbot, Y.; Ben-Shaul, A.; Granek, R.; Gelbart, W. M. *J. Chem. Phys.* **1995**, *103*, 8764.
(58) Drye, T. J.; Cates, M. E. *J. Chem. Phys.* **1992**, *96*, 1367. See also: Karabori, S.; Esselink, K.; Hilbers, P. A. J.; Smit, B.; Karthäuser, J.; van Os, N. M.; Zana, R. *Science (Washington, D.C.)* **1994**, *266*, 254.
(59) Porte, G.; Gomati, R.; El Haitamy, O.; Appell, J.; Marignan, J. *J. Phys. Chem.* **1986**, *90*, 5746.
(60) For general discussions of microemulsions see the chapters in ref 35 by: Auvray, L. (Chapter 7); Gompper, G.; Schick, M. (Chapter 8); Safran, S. A. (Chapter 9). See also: Overbeek, J. Th. G. *Faraday Discuss. Chem. Soc.* **1978**, *65*, 7.
(61) de Gennes, P. G.; Taupin, C. *J. Phys. Chem.* **1982**, *86*, 2294. Jauffroy, J.; Levinson, P.; de Gennes, P. G. *J. Phys.* **1982**, *43*, 1241.
(62) For some of the early lattice-type theories of microemulsions see, e.g.: Talmon, Y.; Prager, S. *J. Chem. Phys.* **1978**, *69*, 2984; **1982**, *76*, 1535. Wheeler, J. C.; Widom, B. *J. Am. Chem. Soc.* **1968**, *90*, 3064. Widom, B. *J. Chem. Phys.* **1984**, *81*, 1030; **1986**, *84*, 6943; *Langmuir* **1987**, *3*, 12. Alexander, S. *J. Phys. Lett.* **1978**, *39*, L1. See also: Stockfisch, T. P.; Wheeler, J. C. *J. Chem. Phys.* **1993**, *99*, 6155.
(63) Kahlweit, M. *Science (Washington, D.C.)* **1988**, *240*, 617.
(64) Langevin, D.; Meunier, J. Chapter 10 in ref 35.
(65) Winsor, P. A. *Trans. Faraday Soc.* **1948**, *44*, 376.
(66) Andelman, D.; Cates, M. E.; Roux, D.; Safran, S. A. *J. Chem. Phys.* **1987**, *87*, 7229.
(67) Gompper, G.; Shick, M. In *Phase Transitions and Critical Phenomena*; Domb, C., Lebowitz, J., Eds.; Academic Press: London, 1994.
(68) Strey, R. *Colloid. Polym. Sci.* **1994**, *272*, 1005.
(69) (a) Pieruschka, P.; Marcelja, S. *Langmuir* **1994**, *10*, 345; *J. Phys. II* **1992**, 235. (b) Pieruschka, P.; Safran, S. A. *Europhys. Lett.* **1993**, *22*, 625.
(70) Helfrich, W. *Z. Naturforsch.* **1973**, *28C*, 693; **1974**, *29C*, 510. Helfrich, W. In *Physics of Defects*; Balian, R., Kleman, M., Poirier, J.-P., Eds.; North-Holland: Amsterdam, 1981. See also: Evans, E. A.; Skalak, R. *CRC Crit. Rev. Bioeng.* **1979**, 181.
(71) Safran, S. A. *Statistical Mechanics of Surfaces, Interfaces and Membranes*; Addison Wesley: Reading, MA, 1994.
(72) Equation 6 is equivalent to the more familiar (Helfrich) form $(f - f_e)/a_0 = (k/2)(c_1 + c_2 - c_0)^2 + \bar{k}c_1c_2$ with $K = k + \bar{k}/2$, $\bar{K} = -\bar{k}/2$, and $c_e = kc_0/(2k + \bar{k})$. k is the *splay* modulus, $\bar{k}$ is the *saddle splay* modulus, and

c_0 is known as the *spontaneous curvature*, a term which we have applied to c_0 (see ref 71).

(73) Safinya, C. R.; Sirota, E. B.; Roux, D.; Smith, G. S. *Phys. Rev. Lett*. **1989**, *62*, 1134. di Meglio, J.-M. In *Physics of Amphiphilic Layers*; Springer Proceedings in Physics Vol. 21; Meunier, J., Langevin, D., Boccara, N., Eds.; Springer: Berlin, 1987; p 153.

(74) Szleifer, I.; Kramer, D.; Ben-Shaul, A.; Gelbart, W. M.; Roux, D. *Phys. Rev. Lett*. **1988**, *60*, 1966. Szleifer, I.; Kramer, D.; Ben-Shaul, A.; Gelbart, W. M.; Safran, S. A. *J. Chem. Phys*. **1990**, *92*, 6800. For a recent review, see: Ben-Shaul, A. Chapter 7 in ref 77.

(75) May, S.; Ben-Shaul, A. *J. Chem. Phys*. **1995**, *103*, 3839.

(76) See, e.g.: Alberts, B.; Bray, D.; Lewis, J.; Raff, M.; Roberts, K.; Watson, J. D. *Molecular Biology of the Cell*, 3rd ed.; Garland Publishing: New York, 1994.

(77) Lipowsky, R.; Sackmann, E., Eds. *Structure and Dynamics of Membranes*; Elsevier: Amsterdam, 1995.

(78) See, for example: Sackmann, E. Chapters 1 and 5 in ref 77. Seifert, U.; Lipowsky, R. Chapter 8 in ref 77.

(79) See, e.g.: Lasic, D. Chapter 10 in ref 77. See also: Lasic, D. *Liposomes: From Physics to Applications*, Elsevier: Amsterdam, 1993.

(80) See, e.g.: Sackmann, E. Chapter 5 in ref 77; see also ref 91.

(81) For recent reviews see, e.g., the chapters in ref 77 by Parsegian, V. A.; Rand, R. P. (Chapter 13); Helfrich, W. (Chapter 14), and Evans, E. (Chapter 15).

(82) Roux, D.; Safinya, C. R.; Nallet, F. Chapter 6 in ref 35.

(83) Roux, D.; Coulon, C.; Cates, M. E. *J. Phys. Chem*. **1992**, *96*, 4174. Cates, M. E. *Physica A* **1991**, *176*, 187. Cates, M. E.; Roux, D.; Andelman, D.; Milner, S. T.; Safran, S. A. *Europhys. Lett*. **1988**, *5*, 733. Bassereau, P.; Marignan, J.; Porte, G. *J. Phys*. **1987**, *48*, 673.

(84) Pieruschka, P. *Phys. Rev. E* **1995**, *52*, 3989. Pieruschka, P.; Safran, S. A. *Europhys. Lett*. **1995**, *31*, 207.

(85) (a) Strey, R.; Schomäker, R.; Roux, D.; Nallet, F.; Olsson, U. *J. Chem. Soc., Faraday Trans*. **1990**, *86*, 2253. (b) Peners, M. H. G. M.; Strey, R. *J. Phys. Chem*. **1995**, *95*, 6091.

(86) See, for example: Seddon, J. M.; Templer, R. H. in ref 77. Lindblom, G.; Rilfors, L. *Biochim. Biophys. Acta* **1989**, *988*, 221. Fontell, K. *Colloid Polym. Sci*. **1990**, *268*, 264.

(87) Lasic, D. D. *Biochem. J*. **1988**, *256*, 1; *Am. Sci*. **1992**, *80*, 20.

(88) Small, D. M. *The Physical Chemistry of Lipids*; Plenum Press: New York, 1986.

(89) Helfrich, W. *J. Phys*. **1986**, *47*, 321.

(90) Ennis, J. *J. Chem. Phys*. **1992**, *97*, 663.

(91) Bloom, M.; Mouritsen, O. G., Chapter 2 in ref 77 and references therein.

(92) Marcelja, S. *Biochim. Biophys. Acta* **1976**, *455*, 1.

(93) Jahnig, F. *Biophys. J*. **1981**, *36*, 329. Abney, J. R.; Owicki, J. C. In *Progress in Protein-Lipid Interactions*; Watts, A., du Pont, J. J. H. H. N., Eds.; Elsevier: Amsterdam, 1985; Chapter 1.

(94) Fattal, D. R.; Ben-Shaul, A. *Biophys. J*. **1993**, *65*, 1795. See also: Fattal, D. R.; Ben-Shaul, A. In *Handbook of Nonmedical Applications of Liposomes*; Lasic, D. D., Barenholz, Y., Eds.; CRC Press: Bocca Raton, FL, 1995; Vol. 1, Chapter 5.

(95) Dan, N.; Pincus, P.; Safran, S. A. *Langmuir* **1993**, *9*, 2768. Dan, N.; Berman, A.; Pincus, P.; Safran, S. A. *J. Phys. II* **1994**, *4*, 1713.

(96) Safran, S. A.; Pincus, P.; Andelman, D. *Science (Washington, D.C.)* **1990**, *248*, 354. MacKintish, F. C.; Safran, S. A. *Phys. Rev. E* **1993**, *47*, 1180.

(97) Yuet, P. K.; Blankschtein, D. *Molecular-Thermodynamic Modeling of Mixed Cationic/Anionic Vesicles* (preprint).

(98) Kaler, E. W.; Murthy, A. K.; Rodriguez, B. E.; Zasadzinski, J. A. N. *Science (Washington, D.C.)* **1989**, *245*, 1371. Kaler, E. W.; Herrington, K. L.; Murthy, A. K.; Zasadzinski, J. A. N. *J. Phys. Chem*. **1992**, *96*, 6698.

(99) Mui, B. L.-S.; Cullis, P. R.; Evans, E. A.; Madden, T. D. *Biophys. J*. **1993**, *64*, 443.

(100) Weakliem, C. L.; Fujii, G.; Chang, J.-E.; Ben-Shaul, A.; Gelbart, W. M. *J. Phys. Chem*. **1995**, *91*, 7694.

(101) For reviews see, e.g.: Lichtenberg, D. In *Biomembranes, Physical Aspects*; Shinitzki, N., Ed.; VCH: Weinheim, 1993; p 63. Dennis, E. A. *Adv. Colloid Interface Sci*. **1986**, *26*, 155.

(102) Walter, A.; Vinson, P. K.; Kaplun, A.; Talmon, Y. *Biophys. J*. **1991**, *60*, 1315.

(103) Edwards, K.; Almgren, N. *J. Colloid Interface Sci*. **1991**, *147*, 1. Mazer, N. A.; Carey, M. C. *Biochemistry* **1983**, *22*, 426. Pedersen, J. S.; Egelbaaf, S. U.; Schurtenberger, P. *J. Phys. Chem*. **1995**, *99*, 1299.

(104) Noro, M. Unpublished results.

(105) Brust, M.; et al. *J. Chem. Soc., Chem. Commun*. **1994**, 802.

(106) Leff, D. V.; Ohara, P. C.; Heath, J. C.; Gelbart, W. M. *J. Phys. Chem*. **1995**, *99*, 7036.

(107) Ohara, P. C.; Leff, D. V.; Heath, J. C.; Gelbart, W. M. *Phys. Rev. Lett*. **1995**, *75*, 3466.

(108) Piirma, I., Ed. *Emulsion Polymerization*; Academic: New York, 1976.

(109) Candau, F. *Encycl. Polym. Sci. Eng*. **1986**, *9*, 718.

(110) Antonietti, M.; et al. *Macromolecules* **1991**, *24*, 6636; **1992**, *25*, 1139.

(111) Asher, S.; et al. *J. Am. Chem. Soc*. **1994**, *116*, 6739, 6745.

(112) Asher, S.; et al. *Macromolecules* **1995**, *28*, 6533.

(113) Weitz, D. A.; Oliveria, M. *Phys. Rev. Lett*. **1984**, *52*, 1433.

(114) Gopal, A. D.; Durian, D. J. *Phys. Rev. Lett*. **1995**, *75*, 2610.

(115) Durian, D. J. *Phys. Rev. Lett*. **1995**, *75*, 4780.

(116) Okuzono, T.; Kawasaki, K. *Phys. Rev. E* **1995**, *51*, 1246.

(117) Hogen-Esch, T. E.; Amis, E. J. *Trends Polym. Sci*. **1995**, *3*, 98.

(118) Chmelka, B. F.; et al. *Science (Washington, D.C.)* **1995**, *267*, 1138.

JP9606570